Title

Synthesis, Pharmacological Characterization, and Structure–Activity Relationships of Noncanonical Selective Agonists for α7 nAChRs

Journal

Journal of Medicinal Chemistry, 62(22)

ISSN

0022-2623

Authors

Camacho-Hernandez, Gisela Andrea
Stokes, Clare
Duggan, Brendan M
et al.

Publication Date

2019-11-27

DOI

10.1021/acs.jmedchem.9b01467

Peer reviewed

HHS Public Access

Author manuscript

J Med Chem. Author manuscript; available in PMC 2020 December 28.

Published in final edited form as:

J Med Chem. 2019 November 27; 62(22): 10376–10390. doi:10.1021/acs.jmedchem.9b01467.

Synthesis, Pharmacological Characterization, and Structure–Activity Relationships of Noncanonical Selective Agonists for $\alpha 7$ nAChRs

Gisela Andrea Camacho-Hernandez[†], **Clare Stokes**[‡], **Brendan M. Duggan**[†], **Katarzyna Kaczanowska**[†], **Stefania Brandao-Araiza**[†], **Lisa Doan**[†], **Roger L. Papke**[‡], **Palmer Taylor**[*,‡]

[†]Department of Pharmacology, Skaggs School of Pharmacy & Pharmaceutical Sciences, University of California-San Diego, La Jolla, California 92093-0751, United States

[‡]Department of Pharmacology & Therapeutics, University of Florida, P.O. Box 100267, Gainesville, Florida 32610-0267, United States

Abstract

A lack of selectivity of classical agonists for the nicotinic acetylcholine receptors (nAChR) has prompted us to identify and develop a distinct scaffold of $\alpha 7$ nAChR-selective ligands. Noncanonical 2,4,6-substituted pyrimidine analogues were framed around compound 40 for a structure–activity relationship study. The new lead compounds activate selectively the $\alpha 7$ nAChRs with EC_{50}'s between 30 and 140 nM in a PNU-120596-dependent, cell-based calcium influx assay. After characterizing the expanded lead landscape, we ranked the compounds for rapid activation using *Xenopus* oocytes expressing human $\alpha 7$ nAChR with a two-electrode voltage clamp. This approach enabled us to define the molecular determinants governing rapid activation, agonist potency, and desensitization of $\alpha 7$ nAChRs after exposure to pyrimidine analogues, thereby distinguishing this subclass of noncanonical agonists from previously defined types of agonists (agonists, partial agonists, silent agonists, and ago-PAMs). By NMR, we analyzed pK_a values for ionization of lead candidates, demonstrating distinctive modes of interaction for this landscape of ligands.

Graphical Abstract

[*]**Corresponding Author** pwtaylor@ucsd.edu.

Author Contributions

The manuscript was written through input and contributions of all the authors. All the authors have given approval to the final version of the manuscript.

ASSOCIATED CONTENT

Supporting Information

The Supporting Information is available free of charge on the ACS Publications website at DOI: 10.1021/acs.jmed-chem.9b01467.

pK_a analysis and chemical characterization (PDF)

Molecular formula strings (CSV)

The authors declare no competing financial interest.

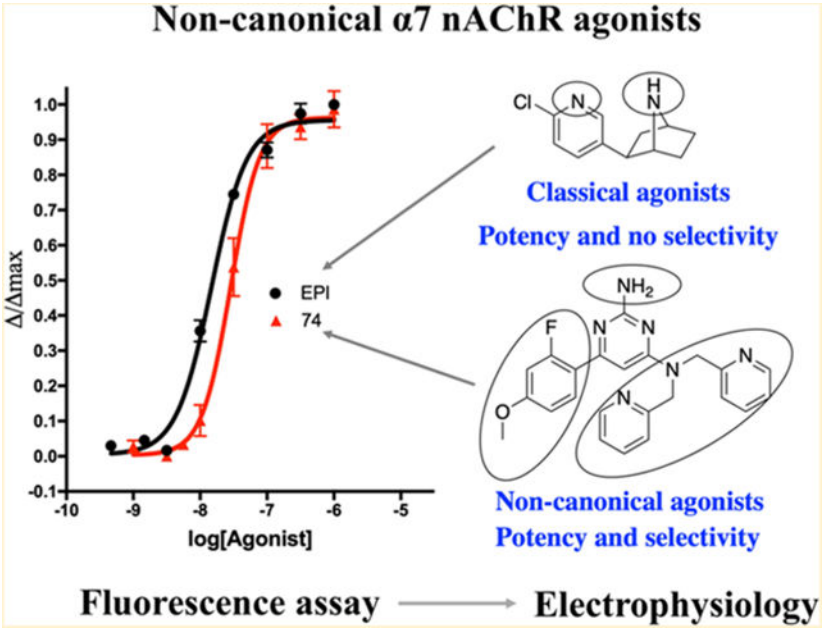

INTRODUCTION

Nicotinic acetylcholine receptors (nAChRs) belong to a pentameric ligand-gated ion channel superfamily and are among the most well-studied allosteric transmembrane signaling proteins.[1,2] They are subclassified as muscle and neuronal receptors, and the latter are widely distributed in the peripheral autonomic and the central nervous systems, as well as in some nonneuronal cell types. nAChRs are predominantly found in brain on presynaptic terminals modulating the release of other neurotransmitters.[3] The orthosteric and allosteric sites and functions of nAChRs have made them potential candidate targets for treating progressive brain disorders of aging and development such as Alzheimer's,[4–6] Parkinson's,[7,8] and schizophrenia,[9,10] as well as inflammation.[11] One of the most abundant neuronal nAChRs is the homopentameric $\alpha 7$ subtype. As such, it is comprised of five identical $\alpha 7$ subunits with five potential orthosteric binding sites, which are located at the respective subunit interfaces of the extracellular domain. The $\alpha 7$ nAChR has unique pharmacological recognition and electrophysiological response properties when compared to other subtypes; for example, it retains relatively low affinity for nicotine or acetylcholine in the desensitized state, is activated by choline, displays high permeability for calcium, and exhibits rapid desensitization when exposed to high concentrations of the agonist.[12,13] The $\alpha 7$ nAChR is highly expressed in the hippocampus and prefrontal cortex, where it modulates cognition, sensory processing, working memory, and attention.[14,15] Activation of this subtype of nAChR can enhance attention and cognition in animal models.[10,15] More recently the $\alpha 7$ nAChR has been explored as a target for inflammation via metabotropic activation in immune cells where it regulates the cholinergic anti-inflammatory pathway.[11,16–18]

Ligand binding to the orthosteric binding site of neuronal and nonneuronal nAChRs requires a cationic center and usually a hydrogen bond donor (HBD) or acceptor (HBA).[19] Horenstein et al. reported three chemical motifs to achieve $\alpha 7$ nAChR selectivity: the

benzylidene motif, tropane motif, and choline motif.[20] Incorporating a hydrophobic feature, such as a single methyl, as with tropane, or a large aromatic group such as the benzylidene in GTS-21,[5,9] in addition to a cationic center can convert a nonselective agonist into a more α7-selective drug. Despite these considerations, more detailed clinical studies have often resulted in leads lacking sufficient selectivity among other nAChR subtypes and a 5-hydroxytryptamine (5-HT_{3A}) ion channel receptor. Accordingly, critical side effects or limited efficacy at the doses used become manifest. GTS-21,[5,9] MEM3454 (RG3487),[15,21] Encenicline (EVP-6124),[22] and TC-5619[10,23] are examples of leads with these characteristics that have been brought to phase 1 and 2 clinical trials (Figure 1).

In previous work,[24] we identified a small subgroup of 4,6-disubstituted-2-aminopyrimidines that interact with the acetylcholine binding protein (AChBP)[25,26] and selectively activate α7 nAChRs in a cell-based calcium influx assay.[27] Moreover, these ligands are structurally distinct from classical nicotinic agonists, where the nitrogens residing on the pyrimidine and pyridine rings all are weakly basic. We hypothesize, based on the structures, when compared to prototypical agonists, that these ligands show limited protonation at physiological pH, thus minimizing classical cation–π interactions.[28] Furthermore, a cell-based calcium influx assay has a prolonged time-frame, so inclusion of a type II positive allosteric modulator (PAM), such as PNU-120596 was required for signal detection. An open question remains as to whether these compounds activate the α7 nAChR in the absence of PNU-120596 and, accordingly, differ from silent agonists[18,29] or ago-PAMs.[30,31] Our current measurements in the oocyte system not only indicate agonist activity without the presence of PNU-120596, but also reveal that the kinetics of activation, efficacy, and recovery from desensitization differ within this pyrimidine subfamily from the classic α7 nAChR agonists described to date.

RESULTS AND DISCUSSION

Synthetic Strategies and Distinguishing Chemistry.

Based on our crystallographic studies with AChBP,[24] in complex with the di(2-picolyl) amine ligand series, we identified key ligand features for influencing AChBP affinity. Along with the di(2-picolyl) amine system capturing the carbonyl and indole regions of Trp143 of *Ls*AChBP, major contributions were attributed to the pyrimidine ring nitrogen and the pyrimidine position 2 NH_2 substituent. With the understanding of importance of the two latter positions, we modified the 2 position by introducing relatively small functional groups with varying electronic influences. Starting with symmetric commercially available pyrimidine precursors, aromatic nucleophilic substitution was performed with 4,6-dichloro-2-(methylthio)pyrimidine, 4,6-dichloropyrimidine, or 4,6-dichloro-2-(trifluoromethyl)pyrimidine to obtain intermediate **B-1** (91% yield), **B-2** (64% yield), or intermediate **B-3** (93% yield), respectively. Crosscoupling Suzuki reactions utilizing a choice of boronic acid, $Pd(dppf)Cl_2$, and as a base K_2CO_3 in *N*,*N*-dimethylacetamide (DMA) yielded compounds **56–59**, **62–63** (Table 1). For compounds **60–61** (Table 1) different coupling conditions were used, namely, $Pd(PPh_3)_4$ as a catalyst, Na_2CO_3 as a base in tetrahydrofuran (THF). A total of eight compounds were synthesized via these two steps.

Compounds **64–65** (Table 1) required an additional oxidation step using *m*-CPBA (Scheme 1).

Recognizing the importance of the di(2-picolyl) amine substituent, we confirmed the need for both pyridines that maintain an axis of symmetry in this part of the structure. Following this concept, we synthesized compound **75** (Scheme 2, Table 1). An additional step was added to assemble *N*-benzyl-1-(pyridin-2-yl)methanamine by a direct reductive amination that afforded **B-4**. Purification of this amine presented a challenge, where the best option seemed to be utilizing oxalic acid to generate the protonated secondary amine. After isolation in 67% yield, the amine was reacted with 2-amino-4,6-dichloropyrimidine to give intermediate **B-5** in 36% yield. Suzuki coupling was performed utilizing $Pd(dppf)Cl_2$ and K_2CO_3 in DMA to yield 83% of a white solid compound **75** (Scheme 2). Based on the previous lead, compound **40**, we continued to expand our landscape with modifications in position 6. Initially, we sampled mostly the -ortho position of the aromatic substituent in combination with different variants of the -para substituents. Our intent was to increase hydrophobicity in this part of the structure, as, according to the earlier studies, this substitution emerged as an important feature to achieve selectivity with respect to other nicotinic receptors.[20] Synthesis of the **B-21** intermediate has been previously described.[24] Coupling condition (b) was utilized to obtain compounds **67–69** (Table 1) and **71–72** (Table 1) in good to excellent yields. In the case of compound **70**, no traces of the expected product were observed leading to reaction condition modification by applying $Pd(PPh_3)_4$ as a catalyst, and Na_2CO_3 as a base in THF. Compound **70** (Table 1) was successfully obtained, albeit in low, 27% yield. Similar coupling conditions were used to produce compounds **73–74** (Table 1).

Because basicity of the pyrimidine nitrogen in the series should be affected by the adjacent substituent in position 6, we introduced a nonaromatic moiety to increase the pK_a in the pyrimidine (calculations performed in MarvinSketch 17.27). Consequently, in compound **66** (Table 1), we introduced morpholine as a substituent via an aromatic substitution performed under microwave irradiation (Scheme 3).[32]

Effects of Divergent Substitutions, Using nAChR Cell-Based Neurotransmitter Fluorescent Engineered Reporters for Structure–Activity Analysis.

As a screen of moderate throughput, and as a first analyzing step, we utilized HEK stable cell lines expressing $\alpha 7$ and $\alpha 4\beta 2$ nAChRs and $5\text{-}HT_{3A}$ receptors with the TN-XXL calcium reporter biosensor.[27] The cell-based neurotransmitter fluorescent-engineered reporters (CNiFERs) measure changes in fluorescence by Ca^{2+} binding as a result of Ca^{2+} influx from agonist activation. Because of the desensitizing profile of $\alpha 7$ nAChR, PNU-120596 was required in initial $\alpha 7$ nAChR screens. Saturation of the genetically encoded fluorescence biosensor can occur, and this may lead to a misinterpretation of efficacy and potency; therefore, we treated this evaluation as a first step to detect well-suited candidates for electrophysiologic analysis.

Out of the 23 present compounds, 19 activated the human $\alpha 7$ nAChRs; accordingly activation was normalized to a 316 nM response of (±)-epibatidine (Figure 2). As a

preliminary structure–activity relationship analysis and to explore how different substitutions in the 2 position affect the response, we compared compound **40**[24] (EC_{50} = 70 nM) with compounds **56** (EC_{50} = 110 nM), **58** (EC_{50} = 140 nM), and 62 (EC_{50} = 530 nM). A decrement of 2- to 8-fold in potency and a modest decrement in the efficacy were observed (Table 1, Figure 2A). In our previous study,[24] utilizing the structural surrogate *Ls*-AChBP in the complex with compound **40** (PDB ID 5j5h), we observed a 2.5–3.5Å hydrogen bonding distance from the conserved Tyr 164 in the α7 nAChR to the NH_2 group. Although the same interaction might not be present in compounds **56** and **58**, compounds **62**, **64**, and **65** should form hydrogen bonds,[33,34] perhaps constrained by parameters of distance, geometry, and molecular dimensions. Compounds **57** (EC_{50} = 1.8 μM), **59** (EC_{50} = 2.1 μM), and **63** (EC_{50} = 2.5 μM), when compared to compound **44**[24] (EC_{50} = 500 nM), present a ~4-fold decrease in potency, underlining sensitivity of this region of the complex and appropriate heterocyclic aromatic group in position 6, and the stabilization by an additional hydrogen bond in position 2 to increase potency. When the aromatic group was replaced by the nonaromatic heterocyclic moiety in **66**, a diminished interaction was detected in all the three different cell lines, despite increased basicity of the pyrimidine ring nitrogen compared to analogs **58–61**, (MarvinSketch pK_a 6.75 for **66**, 4.56 for **58**, 4.71 for **59**, 3.53 for **60**, and 3.48 for **61**). This suggested that basicity of the pyrimidine ring nitrogen does not suffice for this series to maintain affinity/potency to the studied receptors. Rather, the ligand system requires additional hydrophobic interactions offered by aromatic substituents in position 6 of the pyrimidine ring. A similar loss of agonist activity was found by symmetry disruption in the di-2-picolyl system. As demonstrated for compound 75, activation of α7 nAChRs was abolished up to concentrations as high as 13.3 μM, confirming the need for a bidentate system, such as the di(2-picolyl) group, to achieve activation. Interestingly, compound 75 inhibited both $\alpha4\beta2$ nAChR and 5-HT_{3A} receptors. The di(2-picolyl) moiety appears as a key pharmacophore feature for α7 nAChR activation but not necessarily antagonism. When the 2-NH_2 group was replaced by hydrophobic moieties in **56** and **62**, antagonism of $\alpha4\beta2$ nAChR and 5-HT_{3A} serotonin receptors increased. Compounds **64** and **65** exhibited an approximately 7-fold decrease in potency and maintained the selectivity to some degree, suggesting that large polar substituents at position 2 of the pyrimidine reduce potency (Table 1, Figure 2A).

An increase in hydrophobicity and atom size at the -ortho position of the phenyl substituent in position 6 of the pyrimidine ring led to an increment in antagonism of $\alpha4\beta2$ nicotinic and 5-HT_{3A} receptors, as well as a loss in potency in α7 nAChRs (**40** vs **71** and **72**, Table 1, Figure 2B). Substitution with fluorine in compound **74** was aimed at maintaining hydrogen bond accepting properties at the -ortho position while modulating lipophilicity of the ligand. Ligand **74** gave increased potency compared to **41**, with an EC_{50} of 30 nM. The key replacement in compound **74** was a swap of a methoxy group for fluorine. Fluorine can act as a bioisostere of a methoxy group if the binding pocket can accommodate the CH_3 group.[35] A fluorine substitution often leads to improved permeability and metabolic stability, both parameters are of great importance for drug development.[35,36]

Electrophysiological Analysis.

Based on CNiFER results, four compounds were selected for fast activation analysis: compounds **58**, **60**, and **74**, in addition to the previously described[24] compound **40**. Electrophysiological characterization was performed in *Xenopus* oocytes expressing human neuronal $\alpha 7$ nAChR with a two-electrode voltage clamp. Initially, the four compounds were tested at 30 μM (Figure 3); the test responses were normalized to the average of two 60 μM ACh precontrol responses for each oocyte. A single-concentration analysis, when an appropriate concentration is used, can provide information of potency and efficacy based on the peak current to net charge ratio, and facilitates a further concentration-response analysis.[37] The four compounds activated the $\alpha 7$ nAChR at the standard single concentration; peak current measurements were compared, and the responses were significantly larger for all compounds than those for the 60 μM ACh controls (Figure 3), reflecting high potency of the four compounds.[37] After a washing period of 181 s with Ringer's solution, 60 μM ACh was applied, and minimal activation of the receptor was detected for all the compounds (Figure 3), suggesting a low recovery of the receptor and potentially a stabilization of a closed channel, desensitized state. The type II PAM PNU-120596 affects the peak current responses and the kinetics of the agonist response by binding to the transmembrane domain and destabilizing some of the desensitized states.[38] Therefore, to demonstrate whether the pyrimidine analogs induced stabilization of a PAM-sensitive closed, desensitized state (D_s), 10 μM PNU-120596 was applied. As shown in Figure 3, the receptors desensitized by the four compounds responded to PNU-120596, with compounds **58**, **60**, and **74** showing a marked increase over the 60 μM ACh precontrol responses. Despite the stabilization of a PAM-sensitive D_s state by these compounds, thereby resembling silent agonists, the pyrimidines differ by having significant activation when PNU-120596 is absent.

An alternative allosteric binding site in the extracellular vestibule of the $\alpha 7$ nAChR has been suggested to be involved with PNU-dependent reactivation of desensitized receptors.[39] This site was first identified as being one of the two binding sites recognized by the ago-PAM GAT107, the other site being a site in the transmembrane domains that is shared with other PAMs such as PNU-120596 or TQS.[40] A further detailed electrophysiological analysis, outside the scope of the present study, indicates that the 2,4,6-substituted pyrimidine analogues may also depend on this allosteric activation site. Concentration–response curves of selected compounds are shown in Figure 4a, based on the net charge, rather than peak-current, analysis. Because of the rapid desensitization of $\alpha 7$ receptors by high agonist concentrations, peak currents often occur before completing application of the drug, so that increases in the peak current do not reflect increased receptor activation, but rather the synchronization of channel opening events.[41] Net charge analysis avoids this artifact. These results are consistent with single-concentration analysis; compound **74** was the most potent with an EC_{50} of 0.11 ± 0.03 μM and I_{max} = 0.84 ± 0.03 of the ACh maximum, followed by compound **40** with an EC_{50} of 0.35 ± 0.11 μM and I_{max} = 0.98 ± 0.08. Compound **60** showed a partial agonist profile with an EC_{50} of 0.60 ± 0.15 μM and I_{max} = 0.53 ± 0.04.

The least potent compound analyzed electrophysiologically was compound **58**, with an EC_{50} of 3.35 ± 0.68 μM showing a full agonistic profile with an I_{max} = 0.89 ± 0.07. All compounds followed the same potency order in single-concentration analysis and the

calcium CNiFER assay, suggesting that the NH_2 group in position 2 enhances potency. Characterization of the inhibition was made by adding a single concentration of ACh, 60 μM, after application of compounds (Figure 4b). Inhibition followed the potency order: compound **74** with an IC_{50} = 0.47 ± 0.20, **40** IC_{50} = 0.37 ± 0.15, **60** IC_{50} = 1.3 ± 0.30, and **58** IC_{50} = 3.5 ± 1.0 μM, confirming the binding of these compounds in the orthosteric site.

To increase our selectivity profile and confirm previous CNiFER results with the $\alpha4\beta2$ nAChR, all compounds were assayed at 30 μM against four heteromeric receptors: the stoichiometry differing between the human high sensitivity (HS) and low sensitivity (LS) forms of $\alpha4\beta2$[42], $\alpha3\beta4$, and the mouse muscle $\alpha1\beta1\varepsilon\delta$ nAChRs are expressed in *Xenopus* oocytes utilizing the two-electrode voltage clamp system. The four compounds showed high selectivity for the $\alpha7$ subtype with minimal to no activation on heteromeric nAChRs (Figure 5), confirming our previous findings. Compound **40** showed more inhibition of the four receptors when coapplied with ACh, especially in the mouse muscle $\alpha1\beta1\varepsilon\delta$ and human $\alpha3\beta4$ nAChR (Figure 5). Structurally, pyrimidine analogs **40** and **74**, with NH_2 in position 2, appeared to inhibit the $\alpha1\beta1\varepsilon\delta$ and $\alpha3\beta4$ nAChRs more than their two congeners, **58** and **60**. There was no notable preference for inhibition of one of the two isoforms of the $\alpha4\beta2$ nAChR. When recovery of the receptor was assessed by control application of ACh (30 μM for $\alpha1\beta1\varepsilon\delta$, 100 μM for $\alpha3\beta4$, 100 μM for LS $\alpha4\beta2$, and 10 μM for HS $\alpha4\beta2$), $\alpha3\beta4$ and the LS and HS forms of $\alpha4\beta2$ nAChRs appeared to recover faster than the muscle receptor, which remained inhibited after the wash period (Figure 5).

pK_a Determinations and in Silico Physico-chemical Properties.

pK_a values were determined utilizing ^{1}H NMR by measuring chemical shifts when the neighboring nuclei protonate.[43,44] This technique has been reported to be a highly reliable alternative for pK_a assessments when compared to UV-spectroscopy, potentiometric measurements, or in silico estimates.[45,46] Our samples were prepared in phosphate buffer (PB) over pH ranges of 1.85–9.56 for nicotine, 2.62–8.51 for compounds **40** and **74**, and 2.65–7.53 for compound **60**. No D_2O to suppress the H_2O signals was employed to avoid changes in the chemical shifts. Compound **40** was prepared at a final concentration of 1 mM and compounds **60** and **74** at 0.25 mM. Nicotine was used as a control; final concentration over the pH range 9.56–3.28 was 20 mM; 10 mM of nicotine was utilized from pH 3.61 to 1.85. Chemical shifts were plotted against pH forming a sigmoidal curve (Supporting Information). pK_a's were obtained from the inflection points as previously described;[44] pK_a's and standard deviations are reported as means when two or more vicinal hydrogens were plotted. We did not measure the values below pH 2.65 to avoid compound degradation. This did not allow us to reach the plateau of the sigmoidal curve for compound **60** (Supporting Information).

Compounds 40 and 74 containing the 2-amino moiety showed a pKa between 6.85 and 6.68, respectively, from the pyrimidine system; our results argue that only a small fraction of the two compounds will be protonated at physiological pH. When fluorine (compound **74**) was introduced in the orthoposition, a decrease in the pK_a of the vicinal pyrimidine took place, as suggested in previous reports.[36] When the 2-NH_2 entity was substituted by a hydrogen in

compound **60**, the pK_a of the pyrimidine underwent a major drop of ~3.25, underlying the 2-NH_2 entity as a contributor to increase basicity in the pyrimidine system (Table 2).

Two hydrogens of the pyridines in compounds **40** and **74** were followed by NMR. pK_a from the pyridine system in the three compounds varied from 4.1 to 4.3. We compared our results with in silico analysis utilizing Marvin Sketch software.[47] In silico profiles suggested that protonation occur on the endocyclic nitrogens of the pyrimidine system. Previous studies by Schiebel et al.[48] demonstrated protonation by nuclear diffraction, most likely to occur in an endocyclic nitrogen when exocyclic nitrogen is also available. The pK_a's of ionizable moieties in the three compounds exhibited marked differences when compared to nicotine.

Drug-likeliness of analogues **40**, **60**, and **74** was determined in silico utilizing Marvin Sketch software (Table 2).[47] Clog *P*, HBDs and HBAs, and molecular weight (MW) of analyzed analogues are in the range of "Lipinski's rule of 5".[49] The polar surface area (PSA) of 2-NH_2 analogues **40** and **74** increases when compared to that of compound **60**.

CONCLUSIONS

Herein we present the synthesis and pharmacological characterization of a noncanonical structural landscape of ligands for activation of $\alpha 7$ nAChRs that contains a pyrimidine center to which functionalization of positions 2, 4, and 6 was made. Amino substitution in position 2 is important for enhancing activity of the series (Table 1), yet removal or substitution of the 2-amino motif does not eliminate submicromolar agonist responses (Table 1). For the $\alpha 7$ agonist activity a required di(2-picolyl) amine substitution was made at the 4 position of the pyrimidine ring. The symmetry of the di(2-picolyl) amine moiety is critical for activation of the $\alpha 7$ nAChR as seen in compound **75**. Functionalization of aromatic substitution in position 6 plays an important role in modulating the activity and selectivity.

Electrophysiological measurements confirmed activation of the $\alpha 7$ nAChR without the presence of PNU-120596, differing from the responses of silent agonists. Nevertheless, evaluation revealed stabilization of a desensitized PNU-sensitive closed state of the $\alpha 7$ nAChR by the leads. These results, as well as the fact that the structures differ from classical agonists, opens up the possibility of occupation of both the orthosteric and potential allosteric binding sites.[39] A more detailed electrophysiological analysis beyond the scope of this article, directed to the chemical characterization of the series, is necessary to address these alternatives. Nevertheless, it is clear that this family of ligands differ from other agonist classifications in terms of activation and desensitization.

Multiple endocyclic (pyrimidine and pyridine) and exocyclic nitrogens at the 2 and 4 positions are found in this landscape. Our titrations of chemical shifts in ^{1}H NMR reveal that all of the nitrogens exist predominantly as neutral, nonionized species at physiological pH values (Table 2). This contrasts with the classical nicotinic agonists with a separated two ring system, like nicotine, cytisine or epibatidine, one of which contains a strong base and the other a HBD or HBA (Figure 1). It appears from the titration data that the 2-NH_2 group on the pyrimidine will contribute to increasing the basicity in the pyrimidine system (Table 2). In silico analysis utilizing Marvin Sketch (Version 17.27.0) suggests that protonation

may occur at endocyclic nitrogens (Supporting Information), as supported by previously published studies,[48,50] where calculation and nuclear diffraction identified endocyclic nitrogens in 2-aminopyridine and 2-aminopyrimidine as the more stable tautomer. Also, the lack of a dominant cationic species with a high pK_a should facilitate disposition of these compounds at tissue target sites and the potential crossing of the blood–brain barrier to achieve CNS activities and perhaps possible side effects; physicochemical properties of lead compounds are within threshold values for membrane permeation and oral bioavailability.[49,51]

A combination of a screen of moderate throughput, followed by detailed electrophysiological measurements of currents, has enabled us to identify a series of noncanonical selective nAChR agonists. Certainly, this new library of compounds affords some interesting new possibilities and refreshes the concepts of ligand design for nAChRs.

EXPERIMENTAL SECTION

Materials.

Epibatidine (Tocris, batch no. 14B/181649), PNU-120596 (Tocris, batch no. 3A/210007 and 3A/210046), MLA (Tocris, batch no. 20A/164724), 5-HT (Tocris, batch no. 2A/201353 and 2B/226517), tropisetron (Tocris, batch no. 2B/214070), DHβE (Tocris, batch no. 11A/219484), fetal bovine serum (FBS; Gibco, lot: 834471), and glutamine (Gibco, lot: 1894162). Reagents and solvents used for chemical synthesis and for buffer preparation were purchased from commercial sources in the highest purity available and used without further purification. All the final compounds submitted for screening had a purity of 95% or higher [high-performance liquid chromatography–mass spectrometry (HPLC–MS)], and chemical structures were confirmed by ^{1}H and ^{13}C NMR and HRMS (Supporting Information). For NMR assessment a 600 MHz NMR spectrometer and Bruker TopSpin 2.1.6 software was used. An Agilent 1260 liquid chromatography (LC) system coupled with a Thermo LCQdeca mass spectrometer was employed for LC–MS analysis. The electrospray ionization (ESI) source was operated under positive ion mode. An Agilent Zorbax SB-C18 column (ID 4.6 mm × length 150 mm, particle size 3.5 μm) was utilized for LC separation using water with 0.05% trifluoroacetic acid (TFA) as mobile phase A and acetonitrile with 0.05% TFA as mobile phase B. The LC flow rate was set at 1.0 mL/min. The LC gradient setting is as follows: 0 min: 5% mobile phase B, 12 min: 95% mobile phase B, 14 min: 95% mobile phase B, 15 min: 5% mobile phase B, and 20 min: 5% mobile phase B. The total runtime was 20 min. High resolution mass spectrometry (HRMS) data were acquired by using an Agilent 6230 time of flight mass spectrometer with a Jetstream electrospray ionization source.

Syntheses.

6-Chloro-2-(methylthio)-N,N-bis(pyridin-2ylmethyl)-pyrimidin-4-amine (B-1).— Di(2-picolyl)amine (1.12 g, 5.63 mmol) was added to a solution of 4,6-dichloro-2-(methylthio)pyrimidine (1.00 g, 5.01 mmol) and *N*,*N*-diisopropylethylamine (0.73 mL, 5.63 mmol) in DMF (8.0 mL) and the solution was stirred at 80 °C for 3.5 h [reaction was monitored by thin layer chromatography (TLC)]. The solvent was removed under reduced

pressure, brine was added, and the mixture was extracted with ethyl acetate (3 × 40 mL). The organic layers were washed with brine, dried over anhydrous sodium sulfate, and filtered. The filtrate was concentrated on a rotary evaporator, and the product was purified by column chromatography using silica gel (hexanes/EtOAc 3:2) or by crystallization. After purification a white solid was obtained in a 91% yield. ^{1}H NMR (600 MHz, chloroform-*d*): δ 2.37 (s, 3H), 4.74 (s, 2H), 5.14 (s, 2H), 6.22 (s, 1H), 7.26–7.12 (m, 4H), 7.64 (td, J = 7.7, 1.6 Hz, 2H), 8.54 (s, 2H). HR-ESI-TOFMS: $[C_{17}H_{17}ClN_5S]^+$, 358.0885.

6-Chloro-N,N-bis(pyridin-2-ylmethyl)pyrimidin-4-amine (B-2).—Di(2-picolyl)amine (1.45 mL, 8.0 mmol) was added to a solution of 4,6-dichloropyrimidine (1.00 g, 6.70 mmol) and *N,N*-diisopropylethylamine (1.40 mL, 8.00 mmol) in DMF (9.0 mL) and the solution was stirred at 80 °C for 1.5 h (reaction was monitored by TLC). The solvent was removed under reduced pressure, brine was added, and the mixture was extracted with ethyl acetate (3 × 40 mL). The organic layers were washed with brine, dried over anhydrous sodium sulfate, and filtered. The filtrate was concentrated on a rotary evaporator, and the product was purified by column chromatography using silica gel and hexanes/EtOAc (1:3). After purification a white solid was obtained in a 64% yield. ^{1}H NMR (600 MHz, chloroform-*d*): δ 4.77 (s, 2H), 5.12 (s, 2H), 6.54 (s, 1H), 7.30–7.11 (m, 4H), 7.65 (td, J = 7.7, 1.7 Hz, 2H), 8.44 (s, 1H), 8.57 (s, 2H). ^{13}C-APT NMR (151 MHz, chloroform-*d*): δ 53.7 (CH_2), 102.2 (CH), 102.2 (CH), 122.9 (CH), 137.2 (CH), 158.3 (CH), 160.0 (C), 160.3 (C), 163.4 (C). HR-ESI-TOFMS: $[C_{16}H_{15}ClN_5]^+$, 312.1007.

6-Chloro-N,N-bis(pyridin-2-ylmethyl)-2-(trifluoromethyl)-pyrimidin-4-amine (B-3).—Di(2-picolyl)amine (0.22 mL, 1.20 mmol) was added to a solution of 4,6-dichloro-2-(trifluoromethyl)pyrimidine (0.22 g, 1.00 mmol) and *N,N*-diisopropylethylamine (0.21 mL, 1.20 mmol) in DMF (1.5 mL) and the solution was stirred at 80 °C for 3.5 h (reaction monitored by TLC). The solvent was removed under reduced pressure, brine was added, and the mixture was extracted with ethyl acetate (3 × 20 mL). The organic layers were washed with brine, dried over anhydrous sodium sulfate, and filtered. The filtrate was concentrated on a rotary evaporator, and the product was purified by column chromatography using silica gel (hexanes/EtOAc 7:3). After purification a white solid was obtained in a 93% yield. ^{1}H NMR (600 MHz, chloroform-*d*): δ 4.87 (s, 2H), 5.15 (s, 2H), 6.66 (s, 1H), 7.17 (d, J = 7.1 Hz, 1H), 7.26–7.19 (m, 2H), 7.42 (d, J = 7.1 Hz, 1H), 7.70–7.62 (m, 2H), 8.57 (d, J = 38.8 Hz, 2H). ^{13}C-APT NMR (151 MHz, chloroform-*d*): δ 55.2 (CH_2), 104.0 (CH), 116.5–121.95 (q, $^{1}J_{C–F}$ = 276.3 Hz, CF_3), 121.3 (CH), 123.1 (CH), 123.2 (CH), 123.5 (CH), 149.6 (CH), 150.4 (CH), 155.3 (C), 156.5–155.7 (q, $^{2}J_{C–F}$ = 36.96 Hz, C), 156.4 (C), 160.8 (C), 163.6 (C). HR-ESI-TOFMS: $[C_{17}H_{14}ClF_3N_5]^+$, 380.0879. HPLC: 99% pure.

N-Benzyl-1-(pyridin-2-yl)methanamine (B-4).—To a solution of benzylamine (0.54 g, 5.00 mmol) in 4 mL of ethanol, pyridine-2-carboxaldehyde (0.54 g, 5.00 mmol) in 4.0 mL of ethanol was added. The solution was stirred overnight and boiled gently for 30 min. $NaBH_4$ (0.25 g, 6.50 mmol) was slowly added at 0 °C. After 2 h, 7 mL of H_2O was slowly added followed by addition of 20 mL of a saturated solution of NH_4Cl, bringing the solution to pH 7, and the mixture was extracted with ethyl acetate (3 × 30 mL). The filtrate was

concentrated under reduced pressure and the crude oil was purified. Oxalic acid was added (0.64 g, 5.04 mmol) in 15 mL of ethanol. The salt was filtered and dissolved in 20 mL of H_2O followed by addition of NaOH (30%); extractions with EtOAc were made. The organic solvent was removed and B-5 (oil) was isolated in a 67% yield. ^{1}H NMR (600 MHz, chloroform-*d*): δ 2.52 (s, 1H), 3.86 (s, 2H), 3.94 (s, 2H), 7.20–7.14 (m, 1H), 7.26 (t, J = 7.2 Hz, 1H), 7.34 (td, J = 8.4, 7.9, 2.0 Hz, 3H), 7.38 (d, J = 7.5 Hz, 2H), 7.65 (td, J = 7.6, 1.8 Hz, 1H), 8.57 (ddd, J = 4.8, 1.6, 0.8 Hz, 1H). HR-ESI-TOFMS: $[C_{13}H_{15}N_2]^+$, 199.1223.

N^4-Benzyl-6-chloro-N^4-(pyridin-2-ylmethyl)pyrimidine-2,4-diamine (B-5).—*N*-Benzyl-1-(pyridin-2-yl)methanamine (0.50 g, 2.50 mmol) was added to a solution of 2-amino-4,6-dichloropyrimidine (0.37 g, 2.20 mmol) and *N,N*-diisopropylethylamine (0.44 mL, 2.50 mmol) in DMF (3.4 mL) and the solution was stirred at 80 °C overnight. The solvent was removed under reduced pressure, brine was added, and the mixture was extracted with ethyl acetate (3 × 40 mL). The organic layers were washed with brine, dried over anhydrous magnesium sulfate, and filtered. The filtrate was concentrated on the rotary evaporator, and the product was purified by column chromatography using silica gel (EtOAc/MeOH 9:1). After purification a white solid was obtained in a 36% yield. ^{1}H NMR (600 MHz, chloroform-*d*): δ 4.96 (s, 6H), 5.94 (s, 1H), 7.20 (dd, J = 13.8, 6.6 Hz, 3H), 7.28 (t, J = 7.2 Hz, 2H), 7.33 (t, J = 7.3 Hz, 2H), 7.64 (td, J = 7.7, 1.8 Hz, 1H), 8.57 (d, J = 4.3 Hz, 1H). ^{13}C-APT NMR (151 MHz, chloroform-*d*): δ 52.7 (CH_2), 92.8 (CH), 110.4 (CH), 120.2 (CH), 122.6 (CH), 127.7 (CH), 129.0 (CH), 137.1 (CH), 149.8 (CH), 160.6 (C), 162.3 (C), 164.4 (C). HR-ESI-TOFMS: $[C_{17}H_{17}ClN_5]^+$, 326.1165.

6-Chloro-N^4,N^4-bis(pyridin-2-ylmethyl)pyrimidine-2,4-diamine (B-21).—B-21 was synthesized as previously described.[23] Di(2-picolyl)amine (0.44 mL, 2.20 mmol) was added to a solution of 2-amino-4,6-dichloropyrimidine (0.33 g, 2.00 mmol) and *N,N*-diisopropylethylamine (0.38 mL, 2.20 mmol) in DMF (3.0 mL) and the solution was stirred at 80 °C for 3.5 h (reaction monitored by TLC). The solvent was removed under reduced pressure, brine was added, and the mixture was extracted with ethyl acetate (3 × 20 mL). The organic layers were washed with brine, dried over anhydrous sodium sulfate, and filtered. The filtrate was concentrated on a rotary evaporator, and the product was purified by column chromatography using silica gel (hexanes/EtOAc 7:3) or by crystallization (the compound was crystalized using ethyl acetate as solvent). After purification a white solid was obtained in a 63% yield. ^{1}H NMR (600 MHz, chloroform-*d*): δ 4.74 (br s, 2H), 4.99 (s, 4H), 5.94 (s, 1H), 7.12–7.23 (m, 4H), 7.55–7.69 (m, 2H), 8.52–8.57 (d, J = 4.0 Hz, 2H). ^{13}C-APT NMR (150 MHz, chloroform-*d*): δ 53.2 (CH_2), 92.7 (CH), 122.4 (CH), 136.8 (CH), 149.6 (CH), 160.4 (C), 162.1 (C), 164.1 (C), 170.1 (C). HR-ESI-MS: $[C_{16}H_{16}N_6Cl]^+$, 327.1124.

6-(2-Methoxyphenyl)-2-(methylthio)-N,N-bis(pyridin-2-ylmethyl)pyrimidin-4-amine (56).—2-Methoxyphenyl boronic acid (0.59 g, 3.91 mmol) was added to a solution of 6-chloro-2-(methylthio)-*N,N*-bis(pyridin-2-ylmethyl)pyrimidin-4-amine (**B-1**) (1.00 g, 2.80 mmol) in DMA (22 mL), and 2 M aqueous potassium carbonate (4.19 mL) was added following the addition of $Pd(dppf)Cl_2$ (0.20 g, 0.28 mmol). The resulting mixture was stirred in a capped glass vial at 149 °C overnight. The solvent was removed under reduced pressure,

brine was added, and the mixture was extracted with ethyl acetate (3 × 50 mL). The organic layers were dried over anhydrous magnesium sulfate, and filtered. The filtrate was concentrated under reduced pressure, and the crude product was filtered through silica gel and recrystallized in ethyl acetate to give a white solid in a 53% yield. ^{1}H NMR (600 MHz, chloroform-*d*): δ 2.47 (s, 3H), 3.61 (s, 3H), 4.85 (s, 2H), 5.22 (s, 2H), 6.85 (s, 1H), 6.88 (d, *J* = 8.3 Hz, 1H), 7.02 (t, *J* = 7.5 Hz, 1H), 7.20 (dd, *J* = 7.1, 5.1 Hz, 2H), 7.34 (t, *J* = 7.8 Hz, 2H), 7.65 (t, *J* = 7.6 Hz, 2H), 7.93 (dd, *J* = 7.7, 1.7 Hz, 1H), 8.57 (s, 2H). ^{13}C-APT NMR (151 MHz, chloroform-*d*): δ 14.2 (CH_3), 53.6 (CH_2), 55.3 (CH_3), 99.5 (CH), 111.3 (CH), 114.2 (C), 120.0 (CH), 120.9 (CH), 122.3 (CH), 126.9 (C), 130.8 (CH), 130.9 (CH), 136.9 (CH), 157.6 (C), 161.5 (C), 162.0 (C), 170.63 (C). HR-ESI-TOFMS: $[C_{24}H_{24}N_5OS]^+$, 430.1692. HPLC: 99% pure.

2-(Methylthio)-N,N-bis(pyridin-2-ylmethyl)-6-(thiophen-3-yl)-pyrimidin-4-amine (57).—3-Thienylboronic acid (0.04 g, 0.30 mmol) was added to a solution of 6-chloro-2-(methylthio)-*N*,*N*-bis(pyridin-2-ylmethyl)pyrimidin-4-amine (**B-1**) (0.10 g, 0.3 mmol) in DMA (2.0 mL), and 2 M aqueous potassium carbonate (0.3 mL) was added following the addition of Pd(dppf)Cl_2 (22 mg, 0.030 mmol). The resulting mixture was stirred in a capped glass vial at 149 °C overnight. The solvent was removed under reduced pressure, brine was added, and the mixture was extracted with ethyl acetate (3 × 50 mL). The organic layers were dried over anhydrous magnesium sulfate and filtered. The filtrate was concentrated under reduced pressure and the product was isolated by column chromatography on silica gel using a Hex/EtOAc gradient (pale solid, 40% yield). ^{1}H NMR (600 MHz, chloroform-*d*): δ 2.47 (s, 3H), 4.86 (s, 2H), 5.18 (s, 2H), 6.47 (s, 1H), 7.19 (dd, *J* = 7.0, 5.2 Hz, 3H), 7.36–7.26 (m, 2H), 7.49–7.44 (m, 1H), 7.63 (t, *J* = 7.2 Hz, 2H), 7.94 (d, *J* = 2.1 Hz, 1H), 8.57 (s, 2H). ^{13}C-APT NMR (151 MHz, chloroform-*d*): δ 14.2 (CH_3), 53.7 (CH_2), 94.2 (CH), 122.5 (CH), 125.9 (CH), 126.0 (CH), 126.2 (CH), 127.3 (CH), 127.8 (CH), 136.9 (CH), 140.7 (C), 159.1 (C), 162.4 (C), 171.3 (C). HR-ESI-TOFMS: $[C_{21}H_{20}N_5S_2]^+$, 406.1152. HPLC: 95% pure.

6-(3,4-Dimethoxyphenyl)-N^4,N^4-bis(pyridin-2ylmethyl) pyrimi-dine-2,4-diamine (58).—2-Methoxyphenylboronic acid (0.05 g, 0.30 mmol) was added to a solution of 6-chloro-*N*,*N*-bis(pyridin-2-ylmethyl)pyrimidin-4-amine (**B-2**) (0.075 g, 0.24 mmol) in DMA (2.0 mL), and 2 M aqueous potassium carbonate (0.25 mL) was added following the addition of Pd(dppf)Cl_2 (17 mg, 0.024 mmol). The resulting mixture was stirred in a capped glass vial at 149 °C overnight. DMA was removed under reduced pressure, brine was added, and the mixture was extracted with ethyl acetate (3 × 30 mL). The organic layers were dried over anhydrous magnesium sulfate and filtered. The filtrate was concentrated under reduced pressure and the crude product was purified by column chromatography on silica gel with CH_3Cl/MeOH/NH_4OH 100/1.2/0.2 to give the product as a white solid in a 49% yield. ^{1}H NMR (600 MHz, chloroform-*d*): δ 3.62 (s, 3H), 4.95 (s, 3H), 6.92–6.87 (m, 1H), 7.10 (d, *J* = 1.1 Hz, 1H), 7.04 (t, *J* = 8.0 Hz, 1H), 7.20 (dd, *J* = 7.0, 5.3 Hz, 2H), 7.40–7.28 (m, 2H), 7.65 (td, *J* = 7.7, 1.7 Hz, 2H), 7.86 (dd, *J* = 7.7, 1.8 Hz, 1H), 8.58 (d, *J* = 4.4 Hz, 2H), 8.78 (s, 1H). ^{13}C NMR (151 MHz, chloroform-*d*): δ 53.5 (CH_2), 55.4 (CH_3), 103.8 (CH), 111.4 (CH), 121.0 (CH), 122.5 (CH), 127.1 (C), 129.1 (CH), 130.8 (CH), 130.9 (CH), 137.0 (CH),

149.7 (CH), 156.4 (C), 157.4 (C), 158.2 (CH), 161.6 (C), 162.4 (C). HR-ESI-TOFMS: $[C_{23}H_{22}N_5O]^+$, 384.1820. HPLC: 99% pure.

N,N-Bis(pyridin-2-ylmethyl)-6-(thiophen-3-yl)pyrimidin-4-amine (59).—3-Thienylboronic acid (0.08 g, 0.62 mmol) was added to a solution of 6-chloro-*N,N*-bis(pyridin-2-ylmethyl)pyrimidin-4-amine (**B-2**) (0.15 g, 0.62 mmol) in DMA (3.0 mL), and 2 M aqueous potassium carbonate (0.72 mL) was added following the addition of $Pd(dppf)Cl_2$ (35 mg, 0.05 mmol). The resulting mixture was stirred in a capped glass vial at 149 °C overnight. DMA was removed under reduced pressure, brine was added, and the mixture was extracted with ethyl acetate (3 × 30 mL). The organic layers were dried over anhydrous magnesium sulfate and filtered. The compound was purified using silica gel columns Hex/EtOAc 1:4 to give a white solid in a 74% yield. ^{1}H NMR (600 MHz, chloroform-*d*): δ 8.70–8.67 (m, 1H), 8.59 (d, J = 4.4 Hz, 2H), 7.96–7.93 (m, 1H), 7.64 (td, J = 7.7, 1.7 Hz, 2H), 7.48 (dd, J = 5.1, 1.2 Hz, 1H), 7.34 (dd, J = 5.1, 3.0 Hz, 1H), 7.25 (s, 1H), 7.20 (dd, J = 7.1, 5.2 Hz, 3H), 6.78 (s, 1H), 5.08 (d, J = 57.2 Hz, 4H). ^{13}C-APT NMR (151 MHz, chloroform-*d*): δ 53.8 (CH_2), 95.8 (CH), 122.7 (CH), 125.9 (CH), 126.1 (CH), 126.7 (CH), 137.2 (CH), 141.0 (C), 149.9 (C), 158.7 (CH), 159.1 (C), 163.0 (C). HR-ESI-TOFMS: $[C_{20}H_{18}N_5S]^+$, 360.1279. HPLC: 98% pure.

6-(2-Fluoro-4-methoxyphenyl)-N,N-bis(pyridin-2-ylmethyl)-pyrimidin-4-amine (60).—2-Fluoro-4-methoxybenzene boronic acid (0.12 g, 0.67 mmol) was added to a solution of 6-chloro-*N,N*-bis(pyridin-2-ylmethyl)pyrimidin-4-amine (**B-2**) (0.15 g, 0.48 mmol) in THF (3.5 mL), and 2 M aqueous sodium carbonate (0.72 mL) was added following the addition of $Pd(PPh_3)_4$ (0.06 g, 0.048 mmol). The resulting mixture was vigorously stirred in reflux for 6 h. THF was removed under reduced pressure, brine was added, and the mixture was extracted with ethyl acetate (3 × 20 mL). The organic layers were dried over anhydrous magnesium sulfate and filtered. The crude product was purified using biotage ZIP 10 g Si cartridge Hex/EtOAc gradients. A white solid in a 68% yield. ^{1}H NMR (600 MHz, chloroform-*d*): δ 8.74 (s, 1H), 8.59 (d, J = 4.3 Hz, 2H), 8.00 (t, J = 8.9 Hz, 1H), 7.65 (td, J = 7.7, 1.5 Hz, 2H), 7.26 (s, 2H), 7.20 (dd, J =7.0, 5.3 Hz, 2H), 6.97 (s, 1H), 6.79 (dd, J = 8.8, 2.5 Hz, 1H), 6.65–6.59 (m, 1H), 5.14 (s, 4H), 3.83 (s, 3H)·^{13}C-DEPTQ NMR (151 MHz, chloroform-*d*): δ 53.6 (CH_2), 55.8 (CH_3), 102.1–102.3 (d, ^2J = 26.84 Hz, CH), 102.2 (CH), 102.4–102.5 (d, ^4J = 11.54 Hz, CH), 110.5–110.6 (d, ^4J = 2.86 Hz, CH), 118.4–118.5 (d, ^2J = 10.74 Hz, C), 122.6 (CH), 131.5–131.6 (d, ^3J = 4.58 Hz, CH), 137.0 (CH), 149.8 (CH), 158.4 (CH), 159.0 (d, ^3J = 3.08 Hz, C), 160.3 (C), 161.1–162.8 (d, ^1J = 251.79 Hz, C), 162.2–162.3 (d, ^3J = 11.53Hz, C), 162.63 (C). HR-ESI-TOFMS: $[C_{23}H_{21}FN_5O]^+$, 402.1720. HPLC: 95% pure.

6-(2-Fluorophenyl)-N,N-bis(pyridin-2-ylmethyl)pyrimidin-4-amine (61).—2-Fluorophenyl boronic acid (0.13 g, 0.90 mmol) was added to a solution of 6-chloro-*N,N*-bis(pyridin-2-ylmethyl)-pyrimidin-4-amine (**B-2**) (0.2 g, 0.64 mmol) in THF (4.6 mL), and 2 M aqueous sodium carbonate (0.96 mL) was added following the addition of $Pd(PPh_3)_4$ (0.07 g, 0.06 mmol). The resulting mixture was vigorously stirred in reflux overnight. THF was removed under reduced pressure, brine was added, and the mixture was extracted with ethyl acetate (3 × 20 mL). The organic layers were dried over anhydrous magnesium sulfate

and filtered. The crude product was purified using a biotage ZIP 10g Si cartridge and Hex/EtOAc gradients. A white solid in a 81% yield. ^{1}H NMR (600 MHz, chloroform-*d*): δ 8.78 (s, 1H), 8.59 (d, J = 4.5 Hz, 2H), 7.99 (td, J = 7.8, 1.5 Hz, 1H), 7.65 (t, J = 7.6 Hz, 2H), 7.37 (q, J = 7.5, 7.0 Hz, 1H), 7.30–7.17 (m, 5H), 7.09 (dd, J = 11.4, 8.3 Hz, 1H), 7.01 (s, 1H), 5.05 (s, 4H). ^{13}C-DEPTQ NMR (151 MHz, chloroform-*d*): δ 53.6 (CH_2), 103.3–103.4 (d, ^{4}J = 10.17 Hz, CH), 116.3–116.6 (d, ^{2}J 2.88 Hz, CH), 122.6 (CH), 124.6 (d, ^{4}J = 3.66Hz, CH), 126.1–126.2 (d, ^{2}J = 10.68 Hz, C), 130.8–130.9 (d, ^{3}J = 2.6 Hz, CH), 131.4–131.5 (d, ^{3}J = 8.6 Hz, CH), 137.0 (CH), 149.8 (CH), 158.5 (CH), 159.1–159.2 (d, ^{3}J = 2.44 Hz, C), 160.1–161.7 (d, ^{1}J = 251.56 Hz, C), 162.6 (C). HR-ESI-TOFMS: $[C_{22}H_{19}FN_5]^+$, 372.1619. HPLC: 99% pure.

6-(2-Methoxyphenyl)-N,N-bis(pyridin2-ylmethyl)-2-(trifluoromethyl) pyrimidin-4-amine (62).—*2*-Methoxyphenylboronic acid (0.05 g, 0.34 mmol) was added to a solution of 6-chloro-*N,N*-bis(pyridin-2-ylmethyl)-2-(trifluoromethyl)pyrimidin-4-amine (**B-3**) (0.10 g, 0.34 mmol) in DMA (2.0 mL), and 2 M aqueous potassium carbonate (0.20 mL) was added following the addition of Pd(dppf)Cl_2 (19 mg, 0.030 mmol). The resulting mixture was stirred in a capped glass vial at 149 °C overnight. DMA was removed under reduced pressure, brine was added, and the mixture was extracted with ethyl acetate (3 × 30 mL). The organic layers were dried over anhydrous magnesium sulfate and filtered. The filtrate was concentrated under reduced pressure and the crude product was purified by column chromatography on silica gel with Hex/EtOAc 1:4 to give the product as a white solid in a 38% yield. ^{1}H NMR (600 MHz, chloroform-*d*): δ 3.61 (s, 3H), 4.92 (s, 2H), 5.23 (s, 2H), 6.90 (d, J = 8.2 Hz, 1H), 7.05 (t, J = 7.5 Hz, 1H), 7.21 (s, 3H), 7.25 (s, 1H), 7.40–7.33 (m, 1H), 7.52 (s, 1H), 7.67 (s, 2H), 8.02–7.98 (m, 1H), 8.58 (d, J = 25.7 Hz, 2H). ^{13}C-APT NMR (151 MHz, chloroform-*d*): δ 54.26 (CH_2), 55.6 (CH_3), 105.3 (CH), 105.5 (CH), 111.6 (CH), 118.4–121.8 (q, $^{1}J_{C–F}$ = 276.3 Hz, CF_3), 121.3 (CH), 122.8 (CH), 123.0 (CH), 126.1 (C), 131.3 (CH), 131.6 (C), 137.1 (CH), 155.6–156.3 (q, $^{2}J_{C–F}$ = 36.2 Hz, C) 156.2 (CH), 157.8 (C), 161.9 (C), 162.9 (C). HR-ESI-TOFMS: $[C_{24}H_{21}F_3N_5O]^+$, 452.1689. HPLC: 95% pure.

N,N-Bis (pyridin-2-ylmethyl)-6-(thiophen-3-yl)-2-(trifluoromethyl)pyrimidin-4-amine (63).—3-Thienylboronic acid (0.07 g, 0.51 mmol) was added to a solution of 6-chloro-*N,N*-bis(pyridin-2-ylmethyl)-2-(trifluoromethyl)pyrimidin-4-amine (**B-3**) (0.15 g, 0.40 mmol) in DMA (2.6 mL), and 2 M aqueous potassium carbonate (0.59 mL) was added following the addition of Pd(dppf)Cl_2 (29 mg, 0.040 mmol). The resulting mixture was stirred in a capped glass vial at 149 °C for 3.5 h. DMA was removed under reduced pressure, brine was added, and the mixture was extracted with ethyl acetate (3 × 20 mL). The organic layers were dried over anhydrous magnesium sulfate and filtered. Purification, using column chromatography on silica gel (hexanes/EtOAc 1:4), afforded the product (pale solid) in a 95% yield. ^{1}H NMR (600 MHz, chloroform-*d*): δ 8.64–8.50 (m, 2H), 8.03 (dd, J = 3.0, 1.1 Hz, 1H), 7.65 (s, 2H), 7.48 (dd, J = 5.1, 1.1 Hz, 2H), 7.34 (dd, J = 5.1, 3.1 Hz, 1H), 7.21 (dd, J = 7.1, 5.2 Hz, 3H), 6.84 (s, 1H), 5.22 (s, 2H), 4.94 (s, 2H). ^{13}C-DEPTQ NMR (151 MHz, chloroform-*d*): δ 54.0 (CH_2), 99.6 (CH), 116.9–122.4 (C, q, $^{1}J_{C–F}$ = 276.1 Hz, CF_3), 122.7 (CH), 125.7 (CH), 126.5 (CH), 126.8 (CH), 128.5 (CH), 136.9 (CH), 139.7 (C), 145.37

(CH), 155.8–156.5 (C, q $^{2}J_{C–F}$ = 35.5 Hz, CF_3)159.5 (C), 163.1 (C). HR-ESI-TOFMS $[C_{21}H_{17}F_3N_5S]^+$, 428.1152. HPLC: 99% pure.

6-(2-Methoxyphenyl)-2-(methylsulfonyl)-N,N-bis(pyridin-2 ylmethyl)pyrimidin-4-amine (64).—56 (0.30 g, 0.70 mmol) was dissolved in (1.5 mL) DCM, followed by slow addition of *m*-CPBA (0.25 g, 1.50 mmol) at 0 °C. After 3 h, saturated solution of $Na_2S_2O_3$ was added and the mixture was extracted with ethyl acetate (2 × 40 mL). The organic layers were washed with saturated solution of $NaHCO_3$, and the mixture was extracted with ethyl acetate (3 × 40 mL). The organic layers were dried over anhydrous magnesium sulfate and filtered. The filtrate was concentrated under reduced pressure and the crude product was purified by column chromatography on silica gel with Hex/EtOAc 1:4 to give a white solid in a 31% yield. ^{1}H NMR (600 MHz, chloroform-*d*): *δ* 8.59 (d, *J* = 46.9 Hz, 2H), 8.07 (dd, *J* = 7.8, 1.9 Hz, 1H), 7.68 (s, 2H), 7.56 (s, 1H), 7.42–7.38 (m, 1H), 7.37 (s, 1H), 7.26–7.16 (m, 3H), 7.06 (t, *J* = 7.6 Hz, 1H), 6.92 (d, *J* = 8.3 Hz, 1H), 5.24 (s, 2H), 4.96 (s, 2H), 3.64 (s, 3H), 3.29 (s, 3H). ^{13}C-APT NMR (151 MHz, chloroform-*d*): *δ* 38.9 (CH_3), 54.5 (CH_2), 55.5 (CH_3), 105.9 (CH), 111.5 (CH), 120.7 (CH), 121.2 (CH), 123.3 (CH), 125.2 (C), 131.3 (CH), 131.9 (CH), 137.2 (CH), 149.9 (CH), 156.3 (C), 158.0 (C), 161.7 (C), 163.1 (C), 165.0 (C). HR-ESI-TOFMS: $[C_{24}H_{24}N_5O_3S]^+$, 462.1592. HPLC: 95% pure.

6-(2-Methoxyphenyl)-2(methylsulfinyl)-N,N-bis(pyridin-2-ylmethyl)pyrimidin-4-amine (65).—56 (0.10 g, 0.23 mmol) was dissolved in (1.0 mL) DCM, followed by slow addition of *m*-CPBA (0.04g, 0.23 mmol) at 0 °C. After 3 h, a saturated solution of $Na_2S_2O_3$ was added and the mixture was extracted with ethyl acetate (2 × 20 mL). The organic layers were washed with saturated solution of $NaHCO_3$ and the mixture was extracted with ethyl acetate (3 × 20 mL). The organic layers were dried over anhydrous magnesium sulfate and filtered. The filtrate was concentrated under reduced pressure and the crude product was purified by column chromatography on silica gel with EtOAc/MeOH 9:1 to give a white solid in a 79% yield. ^{1}H NMR (600 MHz, chloroform-*d*): *δ* 2.88 (s, 3H) 3.64 (s, 3H), 4.92 (s, 2H), 5.27 (d, *J* = 27.6 Hz, 2H), 6.90 (d, *J* = 8.2 Hz, 1H), 7.04 (t, *J* = 8.0 Hz, 1H), 7.21 (s, 2H), 7.23 (s, 2H), 7.39–7.34 (m, 1H), 7.53 (s, 1H), 7.67 (t, *J* = 7.1 Hz, 2H), 8.06 (dd, *J* = 7.8, 1.8 Hz, 1H), 8.61 (s, 2H)·^{13}C-APT NMR (151 MHz, chloroform-*d*): *δ* 39.9 (CH_3), 54.0 (CH_2), 55.5 (CH_3), 104.2 (CH), 111.5 (CH), 121.2 (CH), 122.7 (CH), 125.8 (C), 131.4 (CH), 131.7 (CH), 137.1 (CH), 157.9 (C), 162.0 (C), 163.2 (C), 172.0 (C). HR-ESI-TOFMS $[C_{24}H_{24}N_5O_2S]^+$, 446.1645. HPLC: 99% pure.

6-Morpholino-N,N-bis(pyridin-2-ylmethyl)pyrimidin-4-amine (66).—To a solution of 6-chloro-*N,N*-bis(pyridin-2-ylmethyl)-pyrimidin-4-amine (**B-2**) (0.15 g, 0.48 mmol) in 2-propanol (0.96 mL), morpholine (0.05 g, 0.57 mmol) and *N,N*-diisopropylethyl-amine (0.12 g, 0.95 mmol) was added. The resulting mixture was stirred in a microwave sealed vial for 20 min at 160 °C. Solvent was removed at reduced pressure, brine was added, and the mixture was extracted with ethyl acetate. The organic layers were dried over anhydrous magnesium sulfate and filtered. The filtrate was concentrated under reduced pressure. The crude product was purified using a biotage ZIP 10 g Si cartridge and Hex/EtOAc gradients. The compound was isolated with EtOAc 100%. Pale powder in a 58% yield. ^{1}H NMR (600

MHz, chloroform-*d*): δ 8.56 (d, J = 4.7 Hz, 2H), 8.29 (s, 1H), 7.64 (td, J = 7.7, 1.6 Hz, 2H), 7.24 (d, J = 7.8 Hz, 2H), 7.19 (dd, J = 7.2, 5.1 Hz, 2H), 5.57 (s, 1H), 4.96 (s, 4H), 3.74–3.69 (m, 4H), 3.46–3.40 (m, 4H). ^{13}C-DEPTQ NMR (151 MHz, chloroform-*d*): δ 44.6 (CH_2), 53.9 (CH_2), 66.7 (CH_2), 81.9 (CH), 121.6 (CH), 122.5 (CH), 137.1 (CH), 149.6 (CH), 157.7 (CH), 158.0 (C), 163.0 (C), 163.5 (C). HR-ESI-TOFMS $[C_{20}H_{23}N_6O]^+$, 363.1930. HPLC: 99% pure.

6-(2-Methoxypyridin-3-yl)-N^4, N^4 -bis(pyridin-2-ylmethyl)-pyrimidine-2,4-diamine (67).—2-Methoxy-3-pyridinephenyl boronic acid (0.11 g, 0.73 mmol) was added to a solution of 6-chloro-N^4,N^4-bis(pyridin-2-ylmethyl)pyrimidine-2,4-diamine (**B-21**) (0.20 g, 0.60 mmol) in DMA (5.0 mL), and 2 M aqueous potassium carbonate (0.92 mL) was added following the addition of Pd(dppf)Cl_2 (45 mg, 0.06 mmol). The resulting mixture was stirred in a capped glass vial at 149 °C for 18 h. DMA was removed under reduced pressure, brine was added, and the mixture was extracted with ethyl acetate (3 × 20 mL). The organic layers were dried over anhydrous magnesium sulfate and filtered. The filtrate was concentrated under reduced pressure and the crude product was isolated by a silica gel column; the compound came out with EtOAc/MeOH 9:1, pale powder, 73% yield. ^{1}H NMR (600 MHz, chloroform-*d*): δ 8.6 (d, J = 4.4 Hz, 2H), 8.2 (d, J = 9.4 Hz, 1H), 8.2 (d, J = 6.9 Hz, 1H), 7.7 (t, J = 8.5 Hz, 2H), 7.3 (s, 2H), 7.2 (dd, J = 7.1, 5.1 Hz, 2H), 7.0 (dd, J = 7.4, 4.9 Hz, 1H), 6.7 (s, 1H), 5.1 (s, 3H), 4.8 (s, 2H), 3.8 (s, 3H). ^{13}C-DEPTQ NMR (151 MHz, chloroform-*d*): δ 53.5 (CH_3), 95.4 (CH), 117.2 (CH), 122.1 (C), 122.3 (CH), 136.9 (CH), 139.1 (CH), 147.4 (CH), 161.1 (C), 161.4 (C), 162.3 (C), 162.8 (C), 163.9 (C). HR-ESI-TOFMS: $[C_{22}H_{22}N_7O]^+$, 400.1883. HPLC: 98% pure.

6-(2,6-Dimethoxyphenyl)-N^4, N^4-bis(pyridin-2-ylmethyl)-pyrimidine-2,4-diamine (68).—2,6-Dimethoxyphenylboronic acid (0.17 g, 0.92 mmol) was added to a solution of 6-chloro-N^4,N^4-bis(pyridin-2-ylmethyl)pyrimidine-2,4-diamine (**B-21**) (0.20 g, 0.61 mmol) in DMA (3.8 mL), and 2 M aqueous potassium carbonate (0.92 mL) was added following the addition of Pd(dppf)Cl_2 (45 mg, 0.06 mmol). The resulting mixture was stirred in a capped glass vial at 149 °C for 24 h. DMA was removed under reduced pressure, brine was added, and the mixture was extracted with ethyl acetate (3 × 30 mL). The organic layers were dried over anhydrous magnesium sulfate and filtered. The crude product was purified using a biotage ZIP 10 g Si cartridge and Hex/EtOAc gradients. Pale powder, 42% yield. ^{1}H NMR (600 MHz, chloroform-*d*): δ 8.5 (d, J = 4.5 Hz, 2H), 7.7 (t, J = 7.2 Hz, 2H), 7.3 (s, 2H), 7.2 (t, J = 8.4 Hz, 1H), 7.19–7.15 (m, 2H), 6.6 (d, J = 8.4 Hz, 2H), 5.9 (s, 1H), 4.9 (s, 4H), 4.8 (s, 2H), 3.7 (s, 6H). ^{13}C-DEPTQ NMR (151 MHz, chloroform-*d*): δ 56.1 (CH_3), 83.9 (C), 96.9 (CH), 104.4 (CH), 107.0 (CH), 122.2 (CH), 129.8 (CH), 132.9 (CH), 136.8 (CH), 157.9 (C), 163.5 (C). HR-ESI-TOFMS: $[C_{24}H_{25}N_6O_2]^+$, 429.2029. HPLC: 99% pure.

6-(4-Fluoro-2-methoxyphenyl)-N^4,N^4-bis(pyridin-2-ylmethyl)-pyrimidine-2,4-diamine (69).—4-Fluoro-2-methoxyphenyl boronic acid (0.104 g, 0.6 mmol) was added to a solution of 6-chloro-N^4,N^4-bis(pyridin-2-ylmethyl)pyrimidine-2,4-diamine (**B-21**) (0.15 g, 0.45 mmol) in DMA (3.0 mL), and 2 M aqueous potassium carbonate (0.35 mL) was added following the addition of Pd(dppf)Cl_2 (22 mg, 0.036 mmol). The resulting mixture was stirred in a capped glass vial at 149 °C overnight. DMA was removed under reduced

pressure, brine was added, and the mixture was extracted with ethyl acetate (3 × 30 mL). The organic layers were dried over anhydrous magnesium sulfate and filtered. The filtrate was concentrated under reduced pressure and the crude product was isolated by silica gel chromatography with Hex/EtOAc gradients to afford a white solid in a 76% yield. ^{1}H NMR (600 MHz, chloroform-*d*): δ 3.6 (s, 3H), 4.8 (s, 6H), 6.4 (s, 1H), 6.6 (dd, *J* = 11.0, 2.4 Hz, 1H), 6.7 (td, *J* = 8.3, 2.4 Hz, 1H), 7.2 (dd, *J* = 7.4, 5.7 Hz, 2H), 7.3 (d, *J* = 30.5 Hz, 2H), 7.6 (td, *J* = 7.7, 1.7 Hz, 2H), 7.7 (dd, *J* = 8.6, 7.1 Hz, 1H), 8.6 (d, *J* = 4.4 Hz, 2H). ^{13}C-APT NMR (151 MHz, chloroform-*d*): δ 55.8 (CH_2), 55.8 (CH_3), 95.5 (CH), 95.5 (CH), 99.7 (CH), 107.4 (CH), 107.6 (CH), 122.4 (CH), 124.2 (C), 131.9 (CH), 132.0 (CH), 137.0 (CH), 149.7 (CH), 158.8 (C), 158.8 (C), 162.4 (C), 162.9 (C), 163.4 (C), 163.7 (C), 165.07 (C). HR-ESI-MS: $[C_{23}H_{22}N_6OF]^+$, 417.1832. HPLC: 100% pure.

6-(2-(Methylthio)phenyl)-N^4, N^4-bis(pyridin-2-ylmethyl)-pyrimidine-2,4-diamine (70).—2-(Methylthio)benzene boronic acid (0.062 g, 0.369 mmol) was added to a solution of 6-chloro-*N*^{4},*N*^{4}-bis(pyridin-2-ylmethyl)pyrimidine-2,4-diamine (**B-21**) (0.1 g, 0.30 mmol) in THF (2.6 mL), and 2 M aqueous sodium carbonate (0.46 mL) was added following the addition of $Pd(PPh_3)_4$ (0.04 g, 0.03 mmol). The resulting mixture was vigorously stirred in reflux overnight. THF was removed under reduced pressure, brine was added, and the mixture was extracted with ethyl acetate (3 × 20 mL). The organic layers were dried over anhydrous magnesium sulfate and filtered. The filtrate was concentrated on a rotary evaporator. The crude product was purified in a silica gel column, using gradients of Hex/EtOAc. Pale powder in a 27% yield. ^{1}H NMR (600 MHz, chloroform-*d*): δ 8.5 (s, 2H), 7.6 (t, *J* = 7.5 Hz, 2H), 7.3 (dd, *J* = 12.0, 7.6 Hz, 4H), 7.2 (d, *J* = 7.9 Hz, 1H), 7.2 (dt, *J* = 15.0, 6.5 Hz, 3H), 6.2 (s, 1H), 5.0 (d, *J* = 104.2 Hz, 3H), 4.8 (s, 3H), 2.3 (s, 3H). ^{13}C-DEPTQ NMR (151 MHz, chloroform-*d*): δ 16.5 (CH_3), 94.8 (CH), 122.4 (CH), 124.8 (CH), 125.8 (CH), 129.3 (CH), 129.4 (CH), 136.9 (CH), 137.5 (C), 139.0 (C), 162.7 (C), 163.7 (C), 166.0 (C). HR-ESI-TOFMS: $[C_{23}H_{23}N_6S]^+$, 415.1701. HPLC: 96% pure.

6-(2-Isopropoxyphenyl)-N4,N4-bis(pyridin-2-ylmethyl)-pyrimidine-2,4-diamine (71).—2-Isopropoxyphenyl boronic acid (0.15 g, 0.85 mmol) was added to a solution of 6-chloro-*N*^{4},*N*^{4}-bis(pyridin-2-ylmethyl)pyrimidine-2,4-diamine (**B-21**) (0.20 g, 0.60 mmol) in DMA (5.0 mL), and 2 M aqueous potassium carbonate (0.91 mL) was added following the addition of $Pd(dppf)Cl_2$ (45 mg, 0.06 mmol). The resulting mixture was stirred in a capped glass vial at 149 °C for 18 h. DMA was removed under reduced pressure, brine was added, and the mixture was extracted with ethyl acetate (3 × 20 mL). The organic layers were dried over anhydrous magnesium sulfate and filtered. The filtrate was concentrated under reduced pressure and the crude product was isolated by a silica gel column, and ethyl acetate was use to isolate it as a pale powder in a 57% of yield. ^{1}H NMR (600 MHz, chloroform-*d*): δ 8.55 (d, *J* = 4.6 Hz, 2H), 7.86 (dd, *J* = 7.7, 1.7 Hz, 1H), 7.64 (t, *J* = 7.5 Hz, 2H), 7.28 (dd, *J* = 15.5, 1.7 Hz, 3H), 7.17 (dd, *J* = 7.1, 5.2 Hz, 2H), 6.99 (t, *J* = 7.5 Hz, 1H), 6.89 (d, *J* = 8.3 Hz, 1H), 6.70 (s, 1H), 5.03 (s, 3H), 4.86 (s, 2H), 4.47 (hept, *J* = 6.0 Hz, 1H), 1.09 (d, *J* = 6.1 Hz, 6H). ^{13}C-DEPTQ NMR (151 MHz, chloroform-*d*): δ 22.0 (CH_3), 70.7 (CH), 95.5 (CH), 114.5 (CH), 120.9 (CH), 122.3 (CH), 128.9 (C), 130.3 (CH), 130.9 (CH), 136.9 (CH), 145.1 (CH), 155.9 (C), 162.8 (C), 163.2 (C), 163.7 (C). HR-ESI-TOFMS: $[C_{25}H_{27}N_6O]^+$, 427.2244. HPLC: 99% pure.

6-(2-Isobutoxyphenyl)-N^4,N^4-bis(pyridin-2-ylmethyl)pyrimidine-2,4-diamine (72).—2-Isobutoxyphenyl boronic acid (0.27 g, 1.37 mmol) was added to a solution of 6-chloro-N^4,N^4-bis(pyridin-2-ylmethyl)pyrimidine-2,4-diamine (**B-21**) (0.3 g, 0.9 mmol) in DMA (7.5 mL), and 2 M aqueous potassium carbonate (1.365 mL) was added following the addition of $Pd(dppf)Cl_2$ (67 mg, 0.09 mmol). The resulting mixture was stirred in a capped glass vial at 149 °C for 3 h. DMA was removed under reduced pressure, brine was added, and the mixture was extracted with ethyl acetate (3 × 20 mL). The organic layers were dried over anhydrous magnesium sulfate and filtered. The filtrate was concentrated under reduced pressure and the crude product was isolated with a silica gel column. The compound came out as a white powder using pure ethyl acetate in a 41% yield. ^{1}H NMR (600 MHz, chloroform-*d*): δ 8.55 (d, J = 4.7 Hz, 2H), 7.78 (dd, J = 7.7, 1.6 Hz, 1H), 7.63 (t, J = 7.7 Hz, 2H), 7.36–7.22 (m, 3H), 7.19–7.14 (m, 2H), 7.00 (t, J = 7.5 Hz, 1H), 6.91–6.86 (m, 1H), 6.64 (s, 1H), 4.96 (s, 3H), 4.81 (s, 2H), 3.68–3.64 (m, 2H), 1.80 (hept, J = 6.6 Hz, 1H). ^{13}C-DEPTQ NMR (151 MHz, chloroform-*d*): δ 19.5 (CH_3), 28.3 (CH), 52.9 (CH_2), 75.1 (CH_2), 95.2 (CH), 112.6 (CH), 120.7 (CH), 122.2 (CH), 128.4 (C), 130.3 (CH), 130.7 (CH), 136.9 (CH), 149.7 (CH), 157.1 (C), 162.8 (C), 163.6 (C), 163.7 (C). HR-ESI-TOFMS: $[C_{26}H_{29}N_6O]^+$, 441.2396. HPLC: 99% pure.

6-(2-Chlorophenyl)-N^4,N^4-bis(pyridin-2-ylmethyl)pyrimidine-2,4-diamine (73).—2-Chlorophenyl boronic acid (0.20 g, 1.28 mmol) was added to a solution of 6-chloro-N^4,N^4-bis(pyridin-2-ylmethyl)-pyrimidine-2,4-diamine (**B-21**) (0.30 g, 0.91 mmol) in THF (7.5 mL), and 2 M aqueous sodium carbonate (1.37 mL) was added following the addition of $Pd(PPh_3)_4$ (0.11 g, 0.09 mmol). The resulting mixture was vigorously stirred in reflux overnight. THF was removed under reduced pressure, brine was added, and the mixture was extracted with ethyl acetate (3 × 30 mL). The organic layers were dried over anhydrous magnesium sulfate and filtered. The filtrate was concentrated on a rotary evaporator. The crude product was purified in a silica gel column, using gradients of Hex/EtOAc. Pale powder, 29% yield. ^{1}H NMR (600 MHz, chloroform-*d*): δ 8.55 (d, J = 4.8 Hz, 2H), 7.64 (t, J = 6.9 Hz, 2H), 7.47 (dd, J = 6.9, 2.4 Hz, 1H), 7.37–7.34 (m, 1H), 7.30–7.24 (m, 4H), 7.19–7.15 (m, 2H), 6.17 (s, 1H), 4.85 (s, 6H). ^{13}C-DEPTQ NMR (151 MHz, chloroform-*d*): δ 95.7 (CH), 122.4 (CH), 127.0 (CH), 128.7 (CH), 129.9 (CH), 130.2 (CH), 130.8 (CH), 132.1 (C), 137.0 (CH), 138.6 (C), 149.7 (CH), 162.8 (C), 163.4 (C), 164.4 (C). HR-ESI-TOFMS: $[C_{22}H_{20}ClN_6]^+$, 403.1429. HPLC 95% pure.

6-(2-Fluoro-4-methoxyphenyl)-N^4,N^4-bis(pyridin-2-ylmethyl)-pyrimidine-2,4-diamine (74).—2-Fluoro-4-methoxybenzene boronic acid (0.22 g, 1.28 mmol) was added to a solution of 6-chloro-N^4,N^4-bis(pyridin-2-ylmethyl)pyrimidine-2,4-diamine (**B-21**) (0.3 g, 0.91 mmol) in THF (7.5 mL), and 2 M aqueous sodium carbonate (1.36 mL) was added following the addition of $Pd(PPh_3)_4$ (0.106 g, 0.09 mmol). The resulting mixture was vigorously stirred in reflux for 8 h. THF was removed under reduced pressure, brine was added, and the mixture was extracted with ethyl acetate (3 × 30 mL). The organic layers were dried over anhydrous magnesium sulfate and filtered. The crude product was purified in a silica gel column, and the compound came out with Hex/EtOAc 1:4. White solid, 74% yield. ^{1}H NMR (600 MHz, chloroform-*d*): δ 8.55 (d, J = 4.3 Hz, 2H), 7.86 (t, J = 8.9 Hz, 1H), 7.63 (t, J = 7.5 Hz, 2H), 7.17 (d, J = 12.1 Hz, 4H), 6.73 (dd, J = 8.8, 2.4 Hz, 1H), 6.58

(dd, J = 13.1, 2.4 Hz, 1H), 6.39 (s, 1H), 4.82 (s, 6H), 3.80 (s, 3H)·^{13}C-DEPTQ NMR (151 MHz, chloroform-d): δ 55.8 (CH_3), 60.6 (CH_2), 94.3–94.4 (d, ^4J = 10.56 Hz, CH), 101.9–102.01 (d, ^2J = 26.85 Hz, CH), 110.3–110.4 (d, ^4J = 2.89 Hz, CH), 119.1–119.2 (d, ^2J = 11.24 Hz, C), 122.4 (CH), 131.3 (d, ^3J = 4.68 Hz, CH), 136.9 (CH), 149.7 (CH), 160.4 (d, ^3J = 2.96 Hz, C), 160.9–162.5 (d, ^1J = 251.41 Hz, C), 161.8 (d, ^3J = 11.36 Hz, C) 162.9 (C), 163.9 (C). HR-ESI-TOFMS: $[C_{23}H_{22}FN_6O]^+$, 417.1829. HPLC: 98% pure.

N^4-Benzyl-6-(2-methoxyphenyl)-N^4-(pyridin-2-ylmethyl)-pyrimidine-2,4-diamine (75).—2-Methoxyphenylboronic acid (0.06 g, 0.37 mmol) was added to a solution of N^4-benzyl-6-chloro-N^4-(pyridin-2-ylmethyl)pyrimidine-2,4-diamine (**B-5**) (0.10 g, 0.30 mmol) in DMA (2.0 mL), and 2 M aqueous potassium carbonate (0.45 mL) was added following the addition of Pd(dppf)Cl_2 (22 mg, 0.030 mmol). The resulting mixture was stirred in a capped glass vial at 149 °C for 3.5 h. DMA was removed under reduced pressure, brine was added, and the mixture was extracted with ethyl acetate (3 × 30 mL). The organic layers were dried over anhydrous magnesium sulfate and filtered. The filtrate was concentrated under reduced pressure and the crude product was filtered through silica gel using ethyl acetate. After purification by column chromatography on silica gel was performed utilizing ethyl acetate to give a white solid in an 83% yield. ^{1}H NMR (600 MHz, DMSO-d_6): δ 8.53 (d, J = 4.3 Hz, 1H), 7.77–7.73 (m, 1H), 7.71–7.68 (m, 1H), 7.33 (q, J = 11.5, 9.7 Hz, 5H), 7.27 (dd, J = 10.4, 5.8 Hz, 3H), 7.02–6.93 (m, 2H), 6.39 (s, 1H), 6.08 (s, 2H), 5.02 (s, 3H), 3.56 (s, 3H). ^{13}C-DEPTQ NMR (151 MHz, DMSO-d_6): δ 55.3 (CH_2), 55.6 (CH_3), 95.74 (CH), 111.6 (CH), 120.2 (CH), 120.2 (CH), 121.0 (CH), 121.5 (CH), 122.0 (CH), 122.3 (CH), 127.4 (CH), 128.4 (C), 128.8 (CH), 130.4 (CH), 130.6 (CH), 137.0 (CH), 145.0 (C), 149.7 (CH), 157.4 (C), 162.9 (C), 163.2 (C), 163.7 (C). HR-ESI-TOFMS: $[C_{24}H_{24}N_5O]^+$, 398.1977. HPLC: 99% pure.

Cell-Based Functional Assays.

Generation of stable cell lines have been previously described[27] to express high levels of the specified receptor and containing the CNiFER were cultured in 10 cm plates with Dulbecco's modified Eagle's media (DMEM; Mediatech, Manassas, VA) supplemented with 10% FBS (Gibco) and 1% Glutamine (Gibco) and incubated at 37 °C with 6% CO_2. Cells were selected at 60% confluency and plated the day before using 100 μL of cell suspension per well into black, transparent flat-bottom, TC-treated 96-well plates (Thermo, Waltham, MA; E&K, Greiner Campbell, CA). On the next day, the media was replaced with 100 μL of artificial cerebrospinal fluid (aCSF, 121 mM NaCl, 5 mM KCl, 26 mM $NaHCO_3$, 1.2 mM $NaH_2PO_4·H_2O$, 10 mM glucose, 2.4 mM $CaCl_2$, 1.3 mM $MgSO_4$, 5 mM HEPES, pH 7.4) buffer for cells expressing $\alpha4\beta2$ and 5-HT_{3A} receptors. For all assays performed on $\alpha7$ nAChR CNiFERs, to aCSF buffer PNU-120596 was added at a 10 μM final concentration. Plates were incubated with the buffer for 30 min at 37 °C and 6% CO_2. Quick screen: the tested compounds were prepared in aCSF for all the receptors except the $\alpha7$ nAChR, where 10 μM PNU-120596, a PAM, was included. The prepared compounds were added in a separate 96-well polypropylene plate (Costar, Corning, NY). Experiments were conducted at 37 °C using a 436 nm excitation wavelength. Emitted light was measured at 485 and 528 nm. Basal fluorescence was recorded for 30 s, followed by addition of 50 μL of the ligand (first addition). Measurements were made at 3.84 s intervals for 2 min to measure the agonist

responses, and then followed by application of the control agonist, which was 100 nM (±)-epibatidine (Tocris Bioscience, Bristol, U.K.) for $\alpha 7$ and $\alpha 4\beta 2$ nAChRs, and 3 μM of 5-hydroxytryptamine (5-HT) (Tocris Bioscience, Bristol, U.K.) for the 5HT3A receptor to evaluate the antagonist responses of the test compounds. Agonist and antagonist properties were screened at a final concentration of 13.3 and 10 μM, respectively. Compounds whose fraction of the maximal response (Δ/Δ_{max}) was higher than 0.20 were further evaluated to determine their EC_{50}, whereas compounds that inhibit Δ/Δ_{max} more than 0.50 were further characterized to determine the type of antagonism and calculate the antagonist dissociation constant (K_A).

Agonist Assays.

Responses were measured in triplicate wells with the FlexStation III (SoftMax Pro 5.2, Molecular Devices) and run at 37 °C by monitoring TN-XXL FRET ratios, emissions of citrine cp174 (527 nm) to eCFP (485 nm), over 120s with agonist injection at 30s. A sigmoidal concentration–response (variable slope) regression of the mean peak FRET ratios was fit to generate concentration–response curves and obtain EC_{50} values (GraphPad Prism 7 for Mac OS X); the plots were normalized to a 316 μM response in the $\alpha 7$ nAChR.

Antagonist Assays.

The tested compounds were prepared in three different concentrations in aCSF; the 96-well plate was divided in four sections (triplicates of each concentration plus the agonist control). The media was replaced by aCSF buffer (first 3 rows) at the 3 concentrations and was incubated for 30 min at 37 °C and 6% CO_2. Agonist was subsequently added and responses were measured in triplicate wells with the FlexStation III (SoftMax Pro 5.2, Molecular Devices) and run at 37 °C by monitoring TN-XXL FRET ratios, emissions of citrine cp174 (527 nm) to eCFP (485 nm), over 120 s with agonist injection at 30 s. A sigmoidal concentration–response (variable slope) regression of the mean peak FRET ratios was fit to generate concentration–response curves of the control agonist, epibatidine for $\alpha 7$ and $\alpha 4\beta 2$ nAChRs, and 5-HT for 5-HT_{3A}. The K_A for competitive antagonists and noncompetitive antagonists were calculated using the next equations.[52]

$$K_A = [A]/[DR - 1] \quad (1)$$

$$K_A = [A]/[\Delta_{max}/\Delta - 1] \quad (2)$$

where [A] is the concentration of the compound, DR (dose ratio) is the EC_{50} ratio of the tested compound over the control compound, which is (±)-epibatidine for the $\alpha 7$ and $\alpha 4\beta 2$ nAChR, and 5HT for $5HT_{3A}$, and Δ/Δ_{max} is the fraction of the maximal response. Mean values and standard deviations were calculated from at least three independent experiments.

Heterologous Expression of nAChRs in *Xenopus* Oocytes.

The cDNA clones of the human nAChR and human resistance-to-cholinesterase 3 (RIC-3) were provided by Dr. Jon Lindstrom (University of Pennsylvania, Philadelphia PA) and Dr. Millet Treinin (Hebrew University, Jerusalem, Israel), respectively. Mouse muscle $\alpha 1$, $\beta 1$,

and δ cDNA clones were provided by Dr. Jim Boulter (Salk Institute, La Jolla CA) and the ε was obtained by Dr. Paul Gardner (University of Massachusetts Medical School, Worcester MA). After linearization and purification of the plasmid cDNAs, RNAs were prepared using the mMessage mMachine in vitro RNA synthesis kit (Ambion, Austin, TX). Oocytes were surgically removed from mature female *Xenopus laevis* frogs (Nasco, Ft. Atkinson, WI) and injected with RNAs of the nAChR and RIC-3 as described previously.[53] The RIC-3 chaperone protein can improve and accelerate α7 expression with no effects on the pharmacological properties of the receptors.[52] Frogs were kept in the Animal Care Service facility of the University of Florida, and all the procedures were approved by the University of Florida Institutional Animal Care and Use Committee. All studies were carried out in accordance with the Guide for the Care and Use of Laboratory Animals as adopted and promulgated by the U.S. National Institutes of Health.

Two-Electrode Voltage-Clamp Electrophysiology of Oocytes.

Experiments were conducted using OpusXpress 6000A (Molecular Devices, Union City, CA).[54] Both the voltage and current electrodes were filled with 3 M KCl. Oocytes were voltage-clamped at −60 mV. The oocytes were bath-perfused with Ringer's solution (115 mM NaCl, 2.5 mM KCl, 1.8 mM $CaCl_2$, 10 mM HEPES, and 1 μM atropine, pH 7.2) with a flow rate of 2 mL/min for α7 and 4 mL/min for the heteromeric nAChR. To evaluate the effects of experimental compounds on nAChRs expressed in oocytes, two initial control responses to applications of ACh were recorded before test applications of experimental drugs alone or coapplied with ACh, and test responses were normalized to the average of the two initial control responses for each oocyte. Drug solutions were applied from a 96-well plate via disposable tips. Drug applications were 12 s long, followed by a 211 s washout period, for α7, and 6 s long, followed by a 271 s washout period, for heteromeric n-AChR. The control concentrations of ACh were 60 μM for wild-type α7, 30 μM for α1β1εδ, 100 μM for α3β4, 100 μM for LS α4β2, and 10 μM for HS α4β2. After experimental drug applications, follow-up control applications of ACh were made to determine primed potentiation, desensitization, or rundown of the receptors. Data were collected at 50 Hz, filtered at 20 Hz (α7) or 5 Hz (heteromeric nAChR), and analyzed by Clampfit 9.2 or 10.0 (Molecular Devices) and Excel (Microsoft, Redmond, WA). Data were expressed as mean ± SEM from at least five oocytes for each experiment and plotted with Kaleidagraph 4.5.2 (Abelbeck Software, Reading, PA). Concentration-response data were fit to the Hill equation using the Levenberg–Marquardt algorithm. Multicell averages were calculated for comparisons of complex responses. Averages of the normalized data were calculated for each of the 10 322 points in each of the 206.44 s traces (acquired at 50 Hz), as well as the SEM for those averages.

pK_a Sample Preparation and ^{1}H NMR Parameters.

We utilized a modified version of a previously reported method by Bezençon et al.[44] Samples were analyzed in 0.1 M PB at various pH between 4.0 and 8.5. Compounds were predissolved in DMSO to a 20 mM concentration. Compound **40** was diluted in PB to a 1 mM final concentration and compounds **60** and **74** to a 0.25 mM final concentration in all pH samples. DMSO concentration was 5% or less in every sample. 500 μL of sample was transferred to a 5 mm NMR tube (NORELL) for recording the NMR spectra. To avoid

having to correct the pH for the presence of deuterium, no deuterated solvent was added to the compound solutions. To provide a lock signal for the NMR spectrometer a sealed 1.7 mm capillary tube filled with DMSO-d_6 was placed in the solution inside the 5 mm NMR tube. DMSO in the capillary also acted as a chemical shift reference. The water peak in the ^{1}H NMR spectra was suppressed via presaturation or by using a jump-return pulse sequence.[55,56] Each spectrum was analyzed using Bruker TopSpin 2.1.6. software. The chemical shifts were plotted against pH using GraphPad Prism 7 and the curve was fitted utilizing a sigmoidal concentration–response (variable slope) equation. The inflection point of the sigmoidal curve gave the pK_a of the analyzed ionizable moiety.

Supplementary Material

Refer to Web version on PubMed Central for supplementary material.

ACKNOWLEDGMENTS

We thank Franziska Schnarkowski, Von V Phan, Quynh My Nguyen, Nila Rahmatyan, and Joannie Ho, for insightful discussions and contributions. The UCSD Chemistry and Biochemistry Molecular MS facility. Bobby Lucero and Carlo Ballatore for the use of the microwave for synthetic reactions.

Funding

NIH GM18360, NIH R01 GM57481.

ABBREVIATIONS

nAChR	nicotinic acetylcholine receptor
5-HT	5-hydroxytryptamine
ACh	acetylcholine
AChBP	acetylcholine binding protein
aCSF	artificial cerebrospinal fluid
KA	antagonist dissociation constant
DMEM	Dulbecco’s modified Eagle’s media
EtOAc	ethylacetate
DCM	dichloromethane
DMF	dimethylformamide
DMA	*N,N*-dimethylacetamide
DMSO	dimethylsulfoxide
DIPEA	*N,N*-diisopropylethylamine
***m*-CPBA**	*meta*-chloroperbenzoic acid

THF	tetrahydrofuran
LS	low sensitivity
HS	high sensitivity
$Pd(dppf)Cl_2$	[1,1′-bis(diphenylphosphino)ferrocene]dichloropalladium(II)
$Pd(PPh_3)_4$	tetrakis(triphenylphosphine)palladium(0)
PAM	positive allosteric modulator
ago-PAM	agonist-positive allosteric modulator
NMR	nuclear magnetic resonance
mm	millimeter
M	molar
μM	micromolar
nM	nanomolar
PB	phosphate buffer
HEK	human embryonic kidney
CNiFERs	cell-based neurotransmitter fluorescent-engineered reporters
^{13}C-DEPTQ	^{13}C-distortionless enhancement by polarization transfer quaternary carbons
^{13}C-APT	^{13}C-attached proton test
HR-ESI-TOFMS	high resolution electrospray ionization time-of-flight mass spectrometry

REFERENCES

(1). Changeux J-P The nicotinic acetylcholine receptor: a typical ‘allosteric machine’. Philo. Trans. R. Soc. Lond B Biol Sci 2018, 373, 20170174.

(2). Taly A; Corringer P-J; Guedin D; Lestage P; Changeux J-P Nicotinic receptors: allosteric transitions and therapeutic targets in the nervous system. Nat. Rev. Drug Discov 2009, 8, 733–750. [PubMed: 19721446]

(3). MacDermott AB; Role LW; Siegelbaum SA Presynaptic ionotropic receptors and the control of transmitter release. Ann. Rev. Neurosci 1999, 22, 443–485. [PubMed: 10202545]

(4). Dziewczapolski G; Glogowski CM; Masliah E; Heinemann SF Deletion of the 7 Nicotinic Acetylcholine Receptor Gene Improves Cognitive Deficits and Synaptic Pathology in a Mouse Model of Alzheimer’s Disease. J. Neurosci 2009, 29, 8805–8815. [PubMed: 19587288]

(5). Kem WR The brain α7 nicotinic receptor may be an important therapeutic target for the treatment of Alzheimer’s disease: studies with DMXBA (GTS-21). Behavioural Brain Research 2000, 113, 169–181. [PubMed: 10942043]

(6). Hoskin JL; Al-Hasan Y; Sabbagh MN Nicotinic acetylcholine receptor agonists for the treatment of Alzheimer's dementia: an update. Nicotine Tob. Res 2019, 21, 370–376. [PubMed: 30137524]

(7). Quik M; Kulak JM Nicotine and nicotinic receptors; relevance to Parkinson's disease. Neurotoxicology 2002, 23, 581–594. [PubMed: 12428730]

(8). Bordia T; Grady SR; McIntosh JM; Quik M. Nigrostriatal Damage Preferentially Decreases a Subpopulation of α6β2* nAChRs in Mouse, Monkey, and Parkinson's Disease Striatum. Mol. Pharmacol 2007, 72, 52–61. [PubMed: 17409284]

(9). Freedman R; Olincy A; Buchanan RW; Harris JG; Gold JM; Johnson L; Allensworth D; Guzman-Bonilla A; Clement B; Ball MP; Kutnick J; Pender V; Martin LF; Stevens KE; Wagner BD; Zerbe GO; Soti F; Kem WR Initial phase 2 trial of a nicotinic agonist in schizophrenia. Am J Psychiatry 2008, 165, 1040–1047. [PubMed: 18381905]

(10). Hauser TA; Kucinski A; Jordan KG; Gatto GJ; Wersinger SR; Hesse RA; Stachowiak EK; Stachowiak MK; Papke RL; Lippiello PM; Bencherif M. TC.−5619: An alpha7 neuronal nicotinic receptor-selective agonist that demonstrates efficacy in animal models of the positive and negative symptoms and cognitive dysfunction of schizophrenia. Biochem. Pharmacol 2009, 78, 803–812. [PubMed: 19482012]

(11). Bagdas D; Gurun MS; Flood P; Papke RL; Damaj MI New Insights on Neuronal Nicotinic Acetylcholine Receptors as Targets for Pain and Inflammation: A Focus on α7 nAChRs. Curr. Neuropharmacol 2018, 16, 415–425. [PubMed: 28820052]

(12). Corradi J; Bouzat C. Understanding the Bases of Function and Modulation of α7 Nicotinic Receptors: Implications for Drug Discovery. Mol. Pharmacol 2016, 90, 288–299. [PubMed: 27190210]

(13). Bertrand D; Lee C-HL; Flood D; Marger F; Donnelly-Roberts D. Therapeutic Potential of α7 Nicotinic Acetylcholine Receptors. Pharmacol. Rev 2015, 67, 1025–1073. [PubMed: 26419447]

(14). Jones S; Sudweeks S; Yakel JL Nicotinic receptors in the brain: correlating physiology with function. Trends Neurosci. 1999, 22, 555–561. [PubMed: 10542436]

(15). Wallace TL; Callahan PM; Tehim A; Bertrand D; Tombaugh G; Wang S; Xie W; Rowe WB; Ong V; Graham E; Terry AV Jr.; Rodefer JS; Herbert B; Murray M; Porter R; Santarelli L; Lowe DA RG3487, a Novel Nicotinic α7 Receptor Partial Agonist, Improves Cognition and Sensorimotor Gating in Rodents. J. Pharmacol. Exp. Ther 2011, 336, 242–253. [PubMed: 20959364]

(16). Kalkman HO; Feuerbach D. Modulatory effects of α7 nAChRs on the immune system and its relevance for CNS disorders. Cell. Mol. Life Sci 2016, 73, 2511–2530. [PubMed: 26979166]

(17). de Jonge WJ; Ulloa L. The alpha7 nicotinic acetylcholine receptor as a pharmacological target for inflammation. Br. J. Pharmacol 2007, 151, 915–929. [PubMed: 17502850]

(18). Horenstein NA; Papke RL Anti-inflammatory silent agonists. ACS Med. Chem. Lett 2017, 8, 989–991. [PubMed: 29057037]

(19). Beers WH; Reich E. Structure and activity of acetylcholine. Nature 1970, 228, 917–922. [PubMed: 4921376]

(20). Horenstein NA; Leonik FM; Papke RL Multiple Pharmacophores for the Selective Activation of Nicotinic α7-Type Acetylcholine Receptors. Mol. Pharmacol 2008, 74, 1496. [PubMed: 18768388]

(21). Umbricht D; Keefe RS; Murray S; Lowe DA; Porter R; Garibaldi G; Santarelli L. A Randomized, Placebo-Controlled Study Investigating the Nicotinic α7 Agonist, RG3487, for Cognitive Deficits in Schizophrenia. Neuropsychopharmacology 2014, 39, 1568–1577. [PubMed: 24549101]

(22). Prickaerts J; van Goethem NP; Chesworth R; Shapiro G; Boess FG; Methfessel C; Reneerkens OAH; Flood DG; Hilt D; Gawryl M; Bertrand S; Bertrand D; König G. EVP-6124, a novel and selective α7 nicotinic acetylcholine receptor partial agonist, improves memory performance by potentiating the acetylcholine response of α7 nicotinic acetylcholine receptors. Neuropharmacology 2012, 62, 1099–1110. [PubMed: 22085888]

(23). Mazurov AA; Kombo DC; Hauser TA; Miao L; Dull G; Genus JF; Fedorov NB; Benson L; Sidach S; Xiao Y; Hammond PS; James JW; Miller CH; Yohannes D. Discovery of (2S,3R)-N-[2-(Pyridin-3-ylmethyl)-1-azabicyclo[2.2.2]oct-3-yl]-benzo[b]furan-2-carboxamide

(TC-5619), a Selective α7 Nicotinic Acetylcholine Receptor Agonist, for the Treatment of Cognitive Disorders. J. Med. Chem 2012, 55, 9793–9809. [PubMed: 23126648]

(24). Kaczanowska K; Camacho Hernandez GA; Bendiks L; Kohs L; Cornejo-Bravo JM; Harel M; Finn MG; Taylor P. Substituted 2-Aminopyrimidines Selective for α7-Nicotinic Acetylcholine Receptor Activation and Association with Acetylcholine Binding Proteins. J. Am. Chem. Soc 2017, 139, 3676–3684. [PubMed: 28221788]

(25). Brejc K; van Dijk WJ; Klaassen RV; Schuurmans M; van Der Oost J; Smit AB; Sixma TK Crystal structure of an ACh-binding protein reveals the ligand-binding domain of nicotinic receptors. Nature 2001, 411, 269–276. [PubMed: 11357122]

(26). Kaczanowska K; Harel M; Radi Z; Changeux J-P; Finn MG; Taylor P. Structural basis for cooperative interactions of substituted 2-aminopyrimidines with the acetylcholine binding protein. Proc. Natl. Acad. Sci. U.S.A 2014, 111, 10749–10754. [PubMed: 25006260]

(27). Yamauchi JG; Nemecz A; Nguyen TQ; Muller A; Schroeder LF; Talley TT; Lindstrom J; Kleinfeld D; Taylor P. Characterizing ligand-gated ion channel receptors with genetically encoded Ca2+ sensors. PLoS One 2011, 6, No. e16519.

(28). Zhong W; Gallivan JP; Zhang Y; Li L; Lester HA; Dougherty DA From ab initio quantum mechanics to molecular neurobiology: A cation-binding site in the nicotinic receptor. Proc. Natl. Acad. Sci. U.S.A 1998, 95, 12088–12093. [PubMed: 9770444]

(29). Quadri M; Matera C; Silnović A; Pismataro MC; Horenstein NA; Stokes C; Papke RL; Dallanoce C. Identification of α7 Nicotinic Acetylcholine Receptor Silent Agonists Based on the Spirocyclic Quinuclidine-Δ2 -Isoxazoline Scaffold: Synthesis and Electrophysiological Evaluation. ChemMedChem 2017, 12, 1335–1348. [PubMed: 28494140]

(30). Papke RL; Horenstein NA; Kulkarni AR; Stokes C; Corrie LW; Maeng C-Y; Thakur GA The Activity of GAT107, an Allosteric Activator and Positive Modulator of α7 Nicotinic Acetylcholine Receptors (nAChR), Is Regulated by Aromatic Amino Acids That Span the Subunit Interface. J. Biol. Chem 2014, 289, 4515–4531. [PubMed: 24362025]

(31). Horenstein NA; Papke RL; Kulkarni AR; Chaturbhuj GU; Stokes C; Manther K; Thakur GA Critical Molecular Determinants of α7 Nicotinic Acetylcholine Receptor Allosteric Activation. J. Biol. Chem 2016, 291, 5049–5067. [PubMed: 26742843]

(32). Luo G; Chen L; Poindexter GS Microwave-assisted synthesis of aminopyrimidines. Tetrahedron Lett. 2002, 43, 5739–5742.

(33). Esterhuysen C; Heßelmann A; Clark T. Trifluoromethyl: An amphiphilic noncovalent bonding partner. ChemPhysChem 2017, 18, 772–784. [PubMed: 28121386]

(34). Eccles KS; Elcoate CJ; Stokes SP; Maguire AR; Lawrence SE Sulfoxides: potent co-crystal formers. Cryst. Growth Des 2010, 10, 4243–4245.

(35). Muller K; Faeh C; Diederich F. Fluorine in pharmaceuticals: looking beyond intuition. Science 2007, 317, 1881–1886. [PubMed: 17901324]

(36). Gillis EP; Eastman KJ; Hill MD; Donnelly DJ; Meanwell NA Applications of fluorine in medicinal chemistry. J. Med. Chem 2015, 58, 8315–8359. [PubMed: 26200936]

(37). Papke RL. Estimation of both the potency and efficacy of α7 nAChR agonists from single-concentration responses. Life Sci. 2006, 78, 2812–2819. [PubMed: 16343553]

(38). Young GT; Zwart R; Walker AS; Sher E; Millar NS Potentiation of 7 nicotinic acetylcholine receptors via an allosteric transmembrane site. Proc. Natl. Acad. Sci. U.S.A 2008, 105, 14686–14691. [PubMed: 18791069]

(39). Gulsevin A; Papke RL; Stokes C; Garai S; Thakur GA; Quadri M; Horenstein NA Allosteric Agonism of α7 Nicotinic Acetylcholine Receptors: Receptor Modulation Outside the Orthosteric Site. Mol. Pharmacol 2019, 95, 606–614. [PubMed: 30944209]

(40). Gill-Thind JK; Dhankher P; D'Oyley JM; Sheppard TD; Millar NS Structurally Similar Allosteric Modulators of α7 Nicotinic Acetylcholine Receptors Exhibit Five Distinct Pharmacological Effects. J. Biol. Chem 2015, 290, 3552–3562. [PubMed: 25516597]

(41). Papke RL; Porter Papke JK Comparative pharmacology of rat and human α7 nAChR conducted with net charge analysis. Br. J. Pharmacol 2002, 137, 49–61. [PubMed: 12183330]

(42). Zhou Y; Nelson ME; Kuryatov A; Choi C; Cooper J; Lindstrom J. Human α4β2 Acetylcholine Receptors Formed from Linked Subunits. J. Neurosci 2003, 23, 9004–9015. [PubMed: 14534234]

(43). Gift AD; Stewart SM; Kwete Bokashanga P. Experimental determination of pKa values by use of NMR chemical shifts, revisited. J. Chem. Educ 2012, 89, 1458–1460.

(44). Bezencon J; Wittwer MB; Cutting B; Smieško M; Wagner B; Kansy M; Ernst B. pK_a determination by ^1H NMR spectroscopy – An old methodology revisited. J. Pharm. Biomed. Anal 2014, 93, 147–155. [PubMed: 24462329]

(45). Babić S; Horvat AJM; Mutavdžić Pavlović D; Kaštelan-Macan M. Determination of pKa values of active pharmaceutical ingredients. TrAC Trends in Analytical Chemistry 2007, 26, 1043–1061.

(46). Kerns EH High throughput physicochemical profiling for drug discovery. J. Pharm. Sci 2001, 90, 1838–1858. [PubMed: 11745742]

(47). In Silico pKa Values Were Calculated Using Marvin Sketch, Version 17.27.0.

(48). Schiebel J; Gaspari R; Sandner A; Ngo K; Gerber H-D; Cavalli A; Ostermann A; Heine A; Klebe G. Charges shift protonation: Neutron diffraction reveals that aniline and 2-amino-pyridine become protonated upon binding to trypsin. Angew. Chem., Int. Ed. Engl 2017, 56, 4887–4890. [PubMed: 28371253]

(49). Lipinski CA; Lombardo F; Dominy BW; Feeney PJ Experimental and computational approaches to estimate solubility and permeability in drug discovery and development settings. Adv. Drug Delivery Rev 1997, 23, 3–25.

(50). Nguyen VQ; Tureček F. Protonation sites in pyrimidine and pyrimidinamines in the gas phase. J. Am. Chem. Soc 1997, 119, 2280–2290.

(51). Veber DF; Johnson SR; Cheng H-Y; Smith BR; Ward KW; Kopple KD Molecular Properties That Influence the Oral Bioavailability of Drug Candidates. J. Med. Chem 2002, 45, 2615–2623. [PubMed: 12036371]

(52). Arunrungvichian K; Fokin VV; Vajragupta O; Taylor P. Selectivity Optimization of Substituted 1,2,3-Triazoles as α7 Nicotinic Acetylcholine Receptor Agonists. ACS Chem. Neurosci 2015, 6, 1317–1330. [PubMed: 25932897]

(53). Halevi S; Yassin L; Eshel M; Sala F; Sala S; Criado M; Treinin M. Conservation within the RIC-3 Gene Family. J. Biol. Chem 2003, 278, 34411–34417. [PubMed: 12821669]

(54). Papke RL; Stokes C. Working with opusxpress: methods for high volume oocyte experiments. Methods 2010, 51, 121–133. [PubMed: 20085813]

(55). Plateau P; Gueron M. Exchangeable proton NMR without base-line distorsion, using new strong-pulse sequences. J. Am. Chem. Soc 1982, 104, 7310–7311.

(56). All Structures Were Drawn Using ChemDraw Professional, version 17.1.1.0.

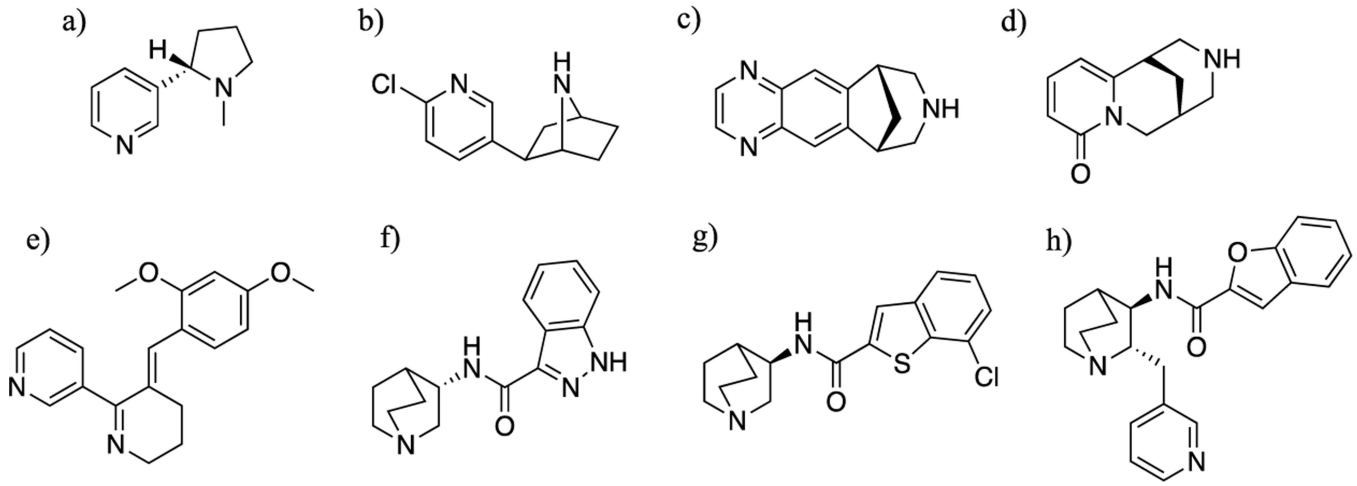

Figure 1.

Examples of nAChR ligands: (a) (–)-nicotine, (b) (±)-epibatidine, (c) varenicline, and (d) cytisine. Examples of nAChR ligands with selective $\alpha 7$ nAChR agonist activation: (e) GTS-21,[5,9] (f) MEM3454 (RG3487),[15,21] (g) encenicline (EVP-6124),[22] (h) TC-5619.[10,23]

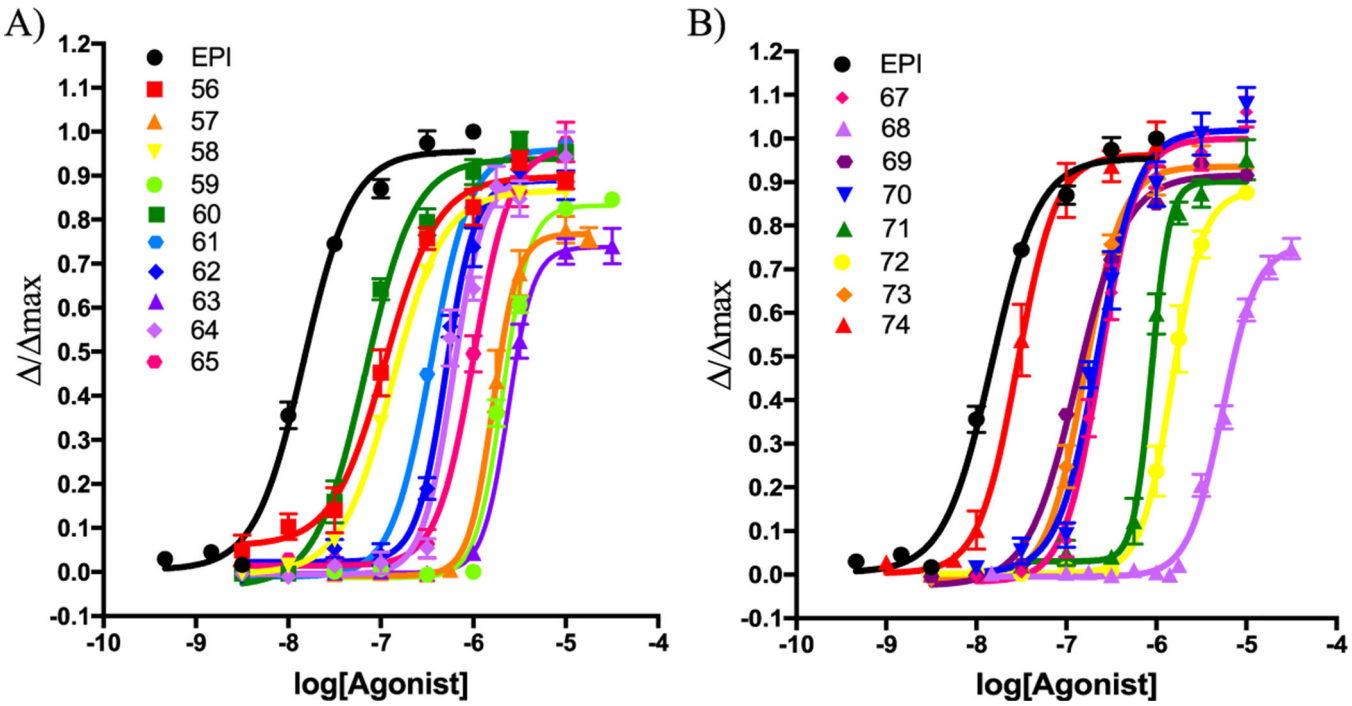

Figure 2.

α7 nAChR concentration–response curves in the presence of PNU-120596 of a series of 2,4,6-trisubstituted pyrimidines performed with HEK cells containing a calcium-sensitive fluorescence reporter.

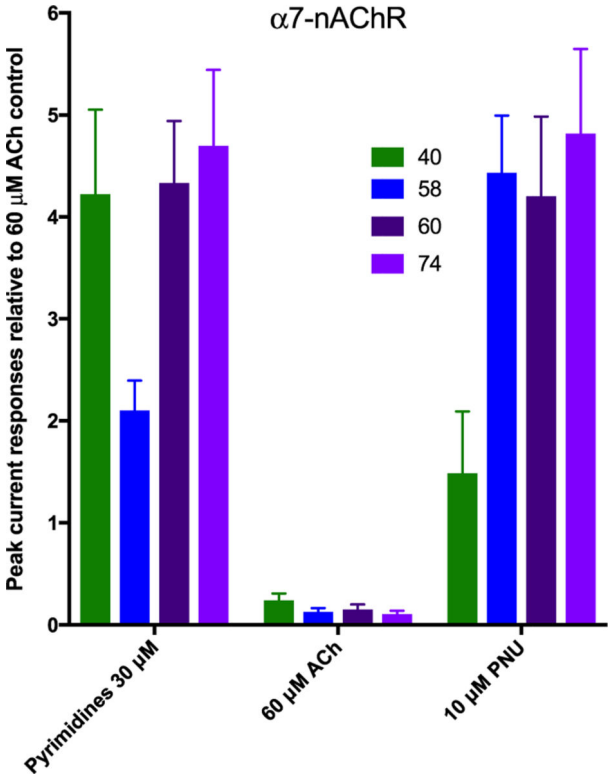

Figure 3.

Peak current responses to 30 μM of selected lead compounds **40**, **58**, **60**, and **74** followed by application of 60 μM ACh and then 10 μM PNU-120596 performed in *Xenopus* oocytes expressing human α7 nAChRs. Compound applications were of a duration of 12 s, followed by 211 s washout periods. Experimental values are the mean responses (±SEM) of six cells, each scaled to their respective ACh precontrols.

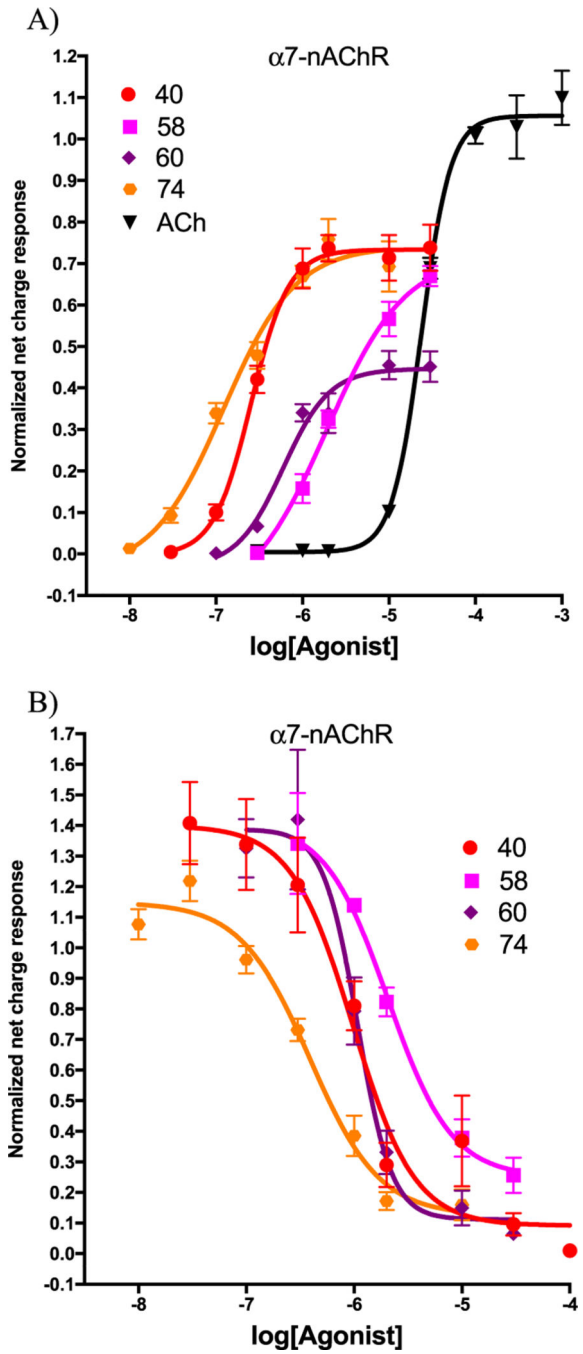

Figure 4.

(a) Concentration–response curves of the $\alpha 7$ nAChR for selected compounds **40**, **58**, **60**, and **74**. The responses are normalized to 60 μM ACh; experimental values are the averaged responses (±SEM) of six cells. (b) Inhibition concentration–response curves of the $\alpha 7$ nAChR for selected compounds **40**, **58**, **60**, and **74**, when tested using 60 μM ACh after application (see Figure 3 for details).

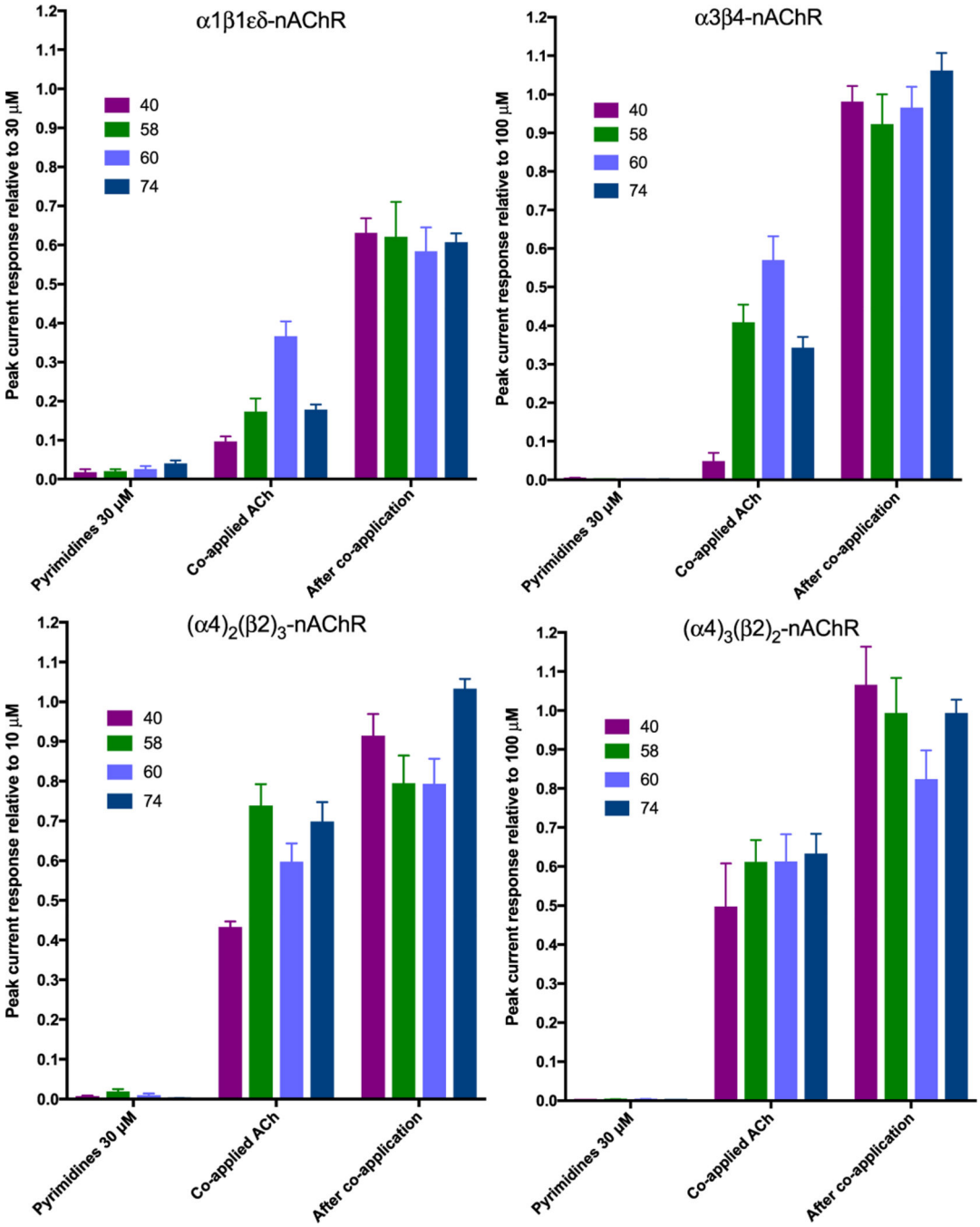

Figure 5.

Electrophysiological evaluation of compounds **40**, **58**, **60**, and **74** in heteropentameric nAChRs performed in *Xenopus* oocytes. Compound applications were of 6 s duration, followed by a 271 s washout period. The control concentrations of ACh were 30 μM for $\alpha 1\beta 1\varepsilon\delta$, 100 μM for $\alpha 3\beta 4$, 100 μM for LS $\alpha 4\beta 2$, and 10 μM for HS $\alpha 4\beta 2$. After experimental drug applications, follow-up control applications of ACh were made to test prior pyrimidine exposures.

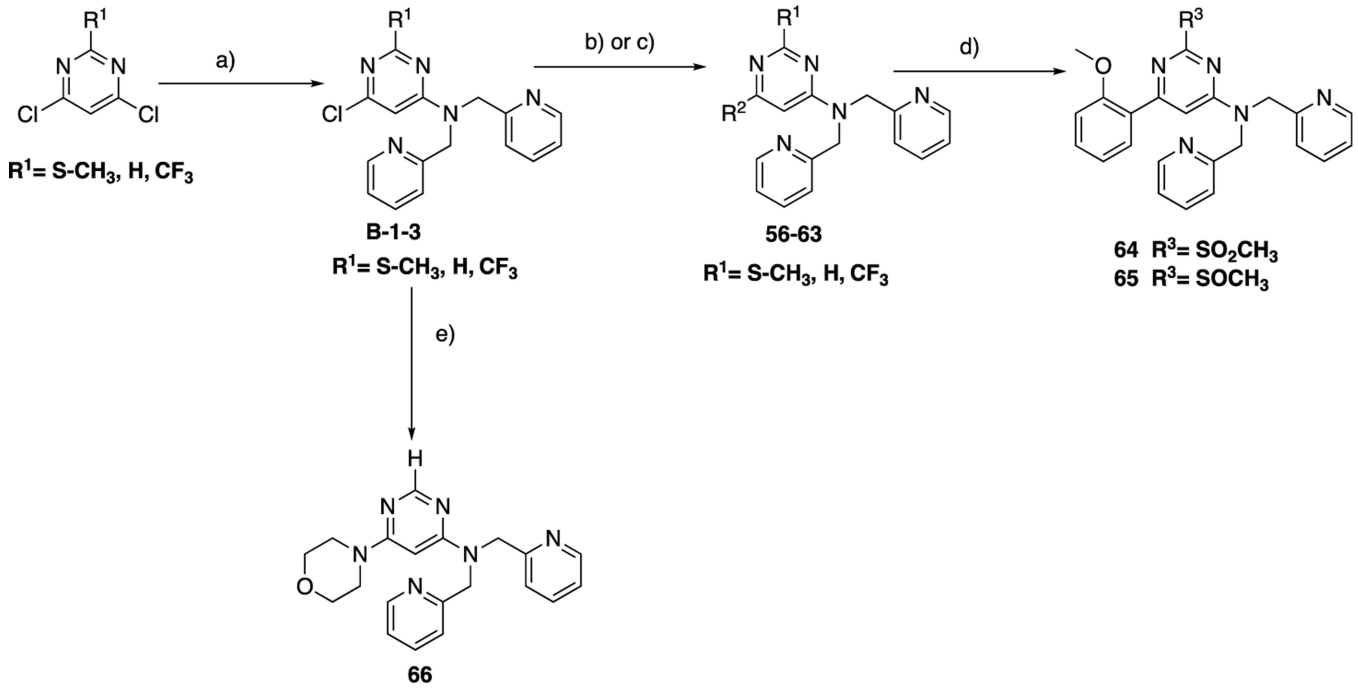

Scheme 1. Synthesis of Compounds 56–66 (for Structures See Table 1)[a]

[a]Reagents and conditions: (a) di(2-picolyl)amine, DIPEA, DMF, 80 °C; (b) boronic acid, $Pd(dppf)Cl_2$, K_2CO_3, DMA, 149 °C; (c) boronic acid, $Pd(PPh_3)_4$, Na_2CO_3, THF, reflux; (d) 1 equiv or 2 equiv of *m*-CPBA in DCM, 0 °C; (e) morpholine, DIPEA, 2-propanol, microwave irradiation, 160 °C.

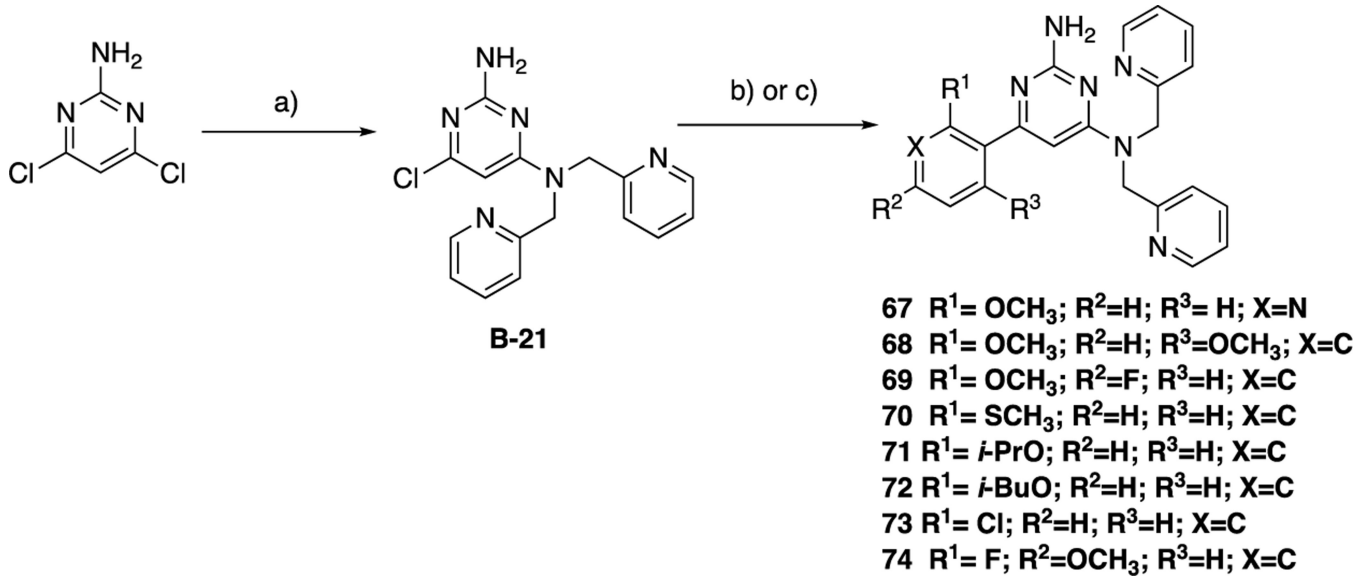

Scheme 2. Modifications at Pyrimidine Position 6[a]

[a]Reagents and conditions: (a) di(2-picolyl amine), DIPEA, DMF, 80 °C; (b) boronic acid, $Pd(dppf)Cl_2$, K_2CO_3, DMA, 149 °C; (c) boronic acid, $Pd(PPh_3)_4$, Na_2CO_3, THF, reflux.

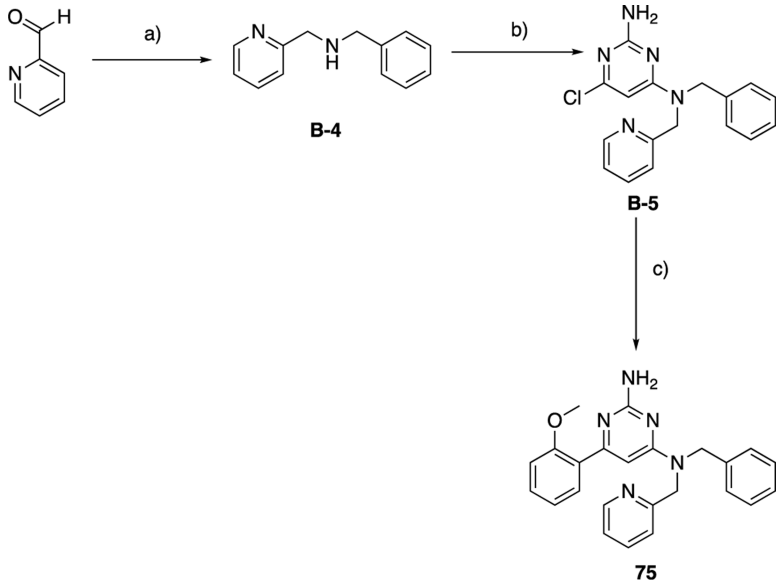

Scheme 3. Modification at Pyrimidine Position 4[a]

[a]Reagents and conditions: (a) benzylamine, $NaBH_4$ EtOH, 0 °C; (b) 2-amino-4,6-dichloropyrimidine, DIPEA, DMF, 80 °C; (c) 2-methoxyphenyl boronic acid, $Pd(dppf)Cl_2$, K_2CO_3, DMA, 149 °C.

Table 1.

Functional Parameters, $\alpha 7$ nAChR EC_{50}, and Antagonist Dissociation Constants, K_A, for $\alpha 4\beta 2$ nAChR and 5-HT_{3A} Receptors[a]

Compound	R¹	R²	R³	Agonist EC_{50} ± SD (μM) α7 nAChR	Antagonist K_A ± SD (μM) α4β2 nAChR	Antagonist K_A ± SD (μM) 5-HT_{3A}
40[b]	NH_2		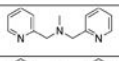	0.07 ± 0.01	6.3 ± 1.5	>10
41[b]	NH_2		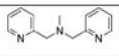	0.07 ± 0.01	2.5 ± 0.8	>10
44[b]	NH_2		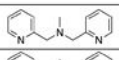	0.5 ± 0.1	>10	>10
56	SCH_3		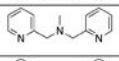	0.11 ± 0.02	1.1 ± 0.2	2.8 ± 0.6
57	SCH_3		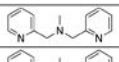	1.8 ± 0.5	3.4 ± 1.5	2.2 ± 0.8
58	H		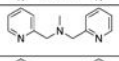	0.14 ± 0.02	7.9 ± 0.9	>10
59	H		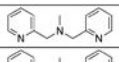	2.1 ± 0.2	>10	>10
60	H		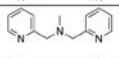	0.069 ± 0.0003	3.0 ± 1.2	5.4 ± 1.1
61	H		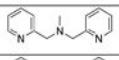	0.36 ± 0.07	5.6 ± 1.1	8.4 ± 1.1
62	CF_3		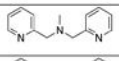	0.53 ± 0.06	1.7 ± 0.3	3.7 ± 0.8
63	CF_3		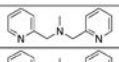	2.5 ± 0.3	0.96 ± 0.2	3.6 ± 1.3
64	SO_2CH_3		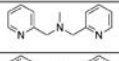	0.69 ± 0.06	7.2 ± 1.9	>10
65	$SOCH_3$		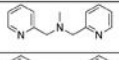	0.92 ± 0.2	>10	>10
66	H		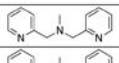	>13.3	>10	>10
67	NH_2		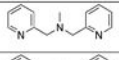	0.23 ± 0.05	>10	>10
68	NH_2		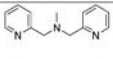	5.4 ± 1.0	7.1 ± 0.9	>10
69	NH_2		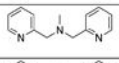	0.12 ± 0.04	4.8 ± 0.8	>10
70	NH_2		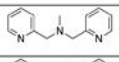	0.24 ± 0.03	4.3 ± 1.5	>10
71	NH_2		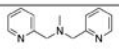	0.89 ± 0.07	1.5 ± 0.4	>10
72	NH_2			1.6 ± 0.5	1.3 ± 0.4	5.5 ± 0.5
73	NH_2			0.16 ± 0.03	3.4 ± 0.9	>10
74	NH_2			0.03±0.009	3.2 ± 1.3	5.3 ± 0.5
75	NH_2			>13.3	1.3 ± 0.6	4.1 ± 0.6

[a] Dissociation constants are based on noncompetitive antagonism. $\alpha 4\beta 2$ nAChR analysis was made without distinguishing subunit stoichiometry. Responses are measured from at least three independent experiments in HEK cells containing a fluorescence reporter and plated as monolayers on a 96-well plate.

[b] Previously described compounds.[24]

Table 2.

pK_a Values for Nicotine and Compounds 40, 60, and 74 Acquired by ^{1}H NMR Spectroscopy and Physicochemical Properties

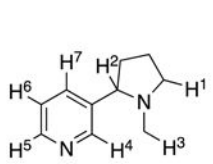

Nicotine

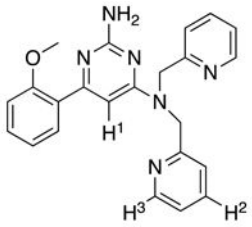

40

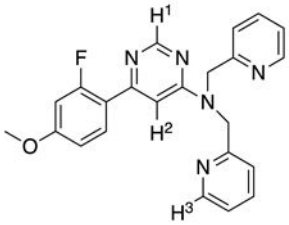

60

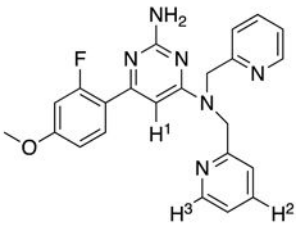

74

compound	^{1}H-NMR pK_a pyrimidine ring mean ± SD	^{1}H-NMR pK_a pyridine ring mean ± SD	^{1}H-NMR pK_a pyrrolidine ring mean ± SD	^{a}pK_a pyrimidine ring	^{a}pK_a pyridine ring	^{a}pK_a pyrrolidine ring	Clog *P*	^{a}HBD	^{a}HBA	^{a}MW	^{a}PSA
nicotine		3.38 ± 0.03	8.17 ± 0.01		2.70	8.58	1.16	0	2	162.12	17.33
40	6.98	4.31 ± 0.02		6.05 (−0.64)	4.39 (4.76)		3.65	1	7	398.19	90.05
60	~3.25	−4.14		3.53 (−1.62)	4.04 (4.53)		3.95	0	6	401.17	60.03
74	6.68	4.26 ± 0.03		5.95 (−0.73)	4.39 (4.75)		3.80	1	7	416.18	90.05

^{a}In silico values calculated utilizing Marvin Sketch software.[47]